STUDIES IN ELECTRON AND X-RAY DIFFRACTION

I
The Structure of Oxygen Fluoride

II
The Failure of the Born Approximation --- The Calculation of Complex Atomic Scattering Amplitudes for Electron Diffraction

III
Some Calculations of Atomic Form Factors

IV
Structural Studies by X-ray Diffraction

Thesis by

James Arthur Ibers

In Partial Fulfillment of the Requirements

for the Degree of

Doctor of Philosophy

California Institute of Technology

Pasadena, California

1954

Acknowledgments

It is a pleasure to acknowledge the encouragement, cooperation, friendship, and acute scientific criticism which Professor Verner Schomaker has provided these past three years. It is likewise a pleasure to acknowledge the encouragement, friendship, advice, and patient instruction which Professor J. Holmes Sturdivant has provided. To these men this thesis belongs.

I should like to acknowledge the friendship and guidance of Professor Norman Davidson both in undergraduate and graduate school. To Professor Davidson I am further indebted for an early and invaluable introduction to scientific research.

I should like to acknowledge the inspiration and friendship which Dr. Jean Hoerni has provided. Collaboration with Dr. Hoerni has been a rich and a rewarding experience.

It is with pleasure that I acknowledge the collaboration of Mr. Gary Felsenfeld in connection with the low-voltage uranium hexafluoride studies.

I should like to acknowledge the splendid cooperation of the Molecular Structure Group. In particular, I should like to acknowledge many helpful discussions with Dr. Richard Marsh, Dr. Kenneth Hedberg, Dr. John Rollett, Dr. David Davies, and Dr. Louis Lavine.

Professor L. Reed Brantley of Occidental College, Professor James C. Warf of the University of Southern California, Professor

H. H. Willard of the University of Michigan, and Dr. Harry Pearlman of North American Aviation Company have been most cooperative in providing samples and special information.

I should like to acknowledge the generosity of the California Institute during undergraduate school, and the generosity of the California Institute, the National Science Foundation, and the General Electric Company during graduate school.

I should like to acknowledge the devotion and understanding of my mother. Her devotion and understanding has made possible my education.

Finally, I should like to acknowledge the love and devotion of my wife, Joyce. Only through her cooperation and encouragement has graduate school been a reality.

Abstract

In Part I the determination of the structure of oxygen fluoride by the method of electron diffraction is described.

In Part II the calculation of complex atomic scattering amplitudes and their use in electron diffraction is discussed. Section A provides an outline of the theory and a summary of the calculations which have been made. In Section B some experimental work, the failure of the Born approximation, and the early calculations are described. In Section C the calculation of complex atomic scattering amplitudes from the partial waves scattering theory and the WKB method is described in detail.

In Part III the calculations of atomic form factors for a few selected atoms from Hartree-Fock and Hartree radial wave functions are described.

In Part IV some structural studies by x-ray diffraction are described. In particular, a determination of the unit cell and space group of tetrapyridinecopper (II) fluoborate is described. A determination of the structure of potassium fluotitanate is presented. Finally, the work to date on the structure of monoclinic ceric iodate is presented. Included in this presentation is a detailed discussion of the various I. B. M. procedures used in the reduction of the large number of intensity data.

Part I

The Structure of Oxygen Fluoride

[Reprinted from the Journal of Physical Chemistry, 57, 699 (1953).]

THE STRUCTURE OF OXYGEN FLUORIDE

BY JAMES A. IBERS[1] AND VERNER SCHOMAKER

Contribution No. 1774 from the Gates and Crellin Laboratories of Chemistry, California Institute of Technology, Pasadena, California

Received January 26, 1953

A bond angle of 103.8 ± 1.5° and a bond length of 1.413 ± 0.019 Å. have been found for oxygen fluoride by the method of electron diffraction. Combining our data with the spectroscopic rotational constant reported by Bernstein and Powling,[2] we arrive at a bond angle of 103.2° and a bond length of 1.418 Å. as most probable values. Special attention was given the problem of weighting the measured ring diameters, and a simple adjustment was finally adopted which may prove useful in other electron diffraction work of this kind.

The bond length and bond angle in oxygen fluoride (OF_2) are of interest, especially in relation to the values for other simple compounds of the electronegative elements, but they have not been precisely determined. The best previous values are dependent on early electron diffraction results and on a single spectroscopically determined molecular constant.

For the present electron diffraction reinvestigation Professor L. Reed Brantley of Occidental College kindly gave us a one-to-one OF_2–O_2 mixture prepared by the usual method.[3] After nearly all the oxygen had been pumped off at liquid-nitrogen temperature,[4] the sample was fractionally distilled at about −160° through a 65-cm. vacuum-jacketed column; iodometric analyses of the product ranged from 98.5 to 99.4 mole % OF_2. Photographs were made and interpreted in the usual way,[5] except that in view of the simplicity of the problem the visual and radial distribution curves were not drawn. The camera distance and electron wave length were 10.91 cm. and 0.06056 Å., respectively.

Intensity curves were calculated for rigid, symmetrical OF_2 models with O—F = 1.42 Å. and F · · · F ranging from 2.10 to 2.32 Å., for various admixtures of O_2. Figure 1 shows three of the curves for pure OF_2 with critical marks[6] to indicate important comparisons with the photographs. The more sensitive features, important for the angle determination, are marked on curves A and C, and the less sensitive features on curve B. Finally, the measured ring positions were compared with

(1) National Science Foundation Predoctoral Fellow, 1952–1953.

(2) H. J. Bernstein and J. Powling, *J. Chem. Phys.*, **18**, 685 (1950).

(3) P. Lebeau and A. Damiens, *Compt. rend.*, **188**, 1253 (1929); O. Ruff and W. Menzel, *Z. anorg. u. allgem. Chem.*, **190**, 257 (1930); G. H. Cady, *J. Am. Chem. Soc.*, **57**, 246 (1935).

(4) The fact that OF_2 can be obtained in about 95% purity by pumping off the oxygen at liquid-nitrogen temperature has been confirmed by the recent work of J. G. Schnizlein, J. L. Sheard, R. C. Toole and T. D O'Brien, THIS JOURNAL, **56**, 233 (1952).

(5) K. Hedberg and A. J. Stosick, *J. Am. Chem. Soc.*, **74**, 954 (1952).

(6) W. F. Sheehan, Jr., and V. Schomaker, *ibid.*, **74**, 4468 (1952).

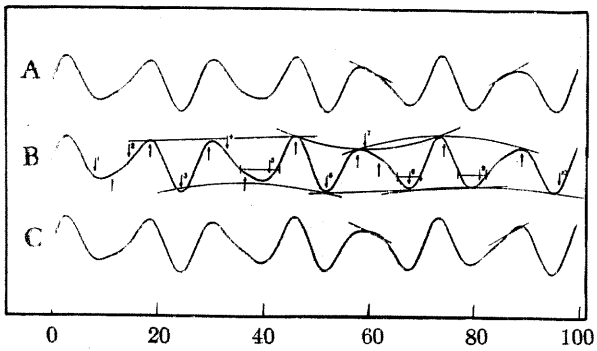

Fig. 1.—Theoretical intensity curves for rigid, symmetrical models of OF_2 with the O—F distance 1.42 Å. and the indicated bond angles: A, 102.8°; B, 103.8°; C, 104.8°.

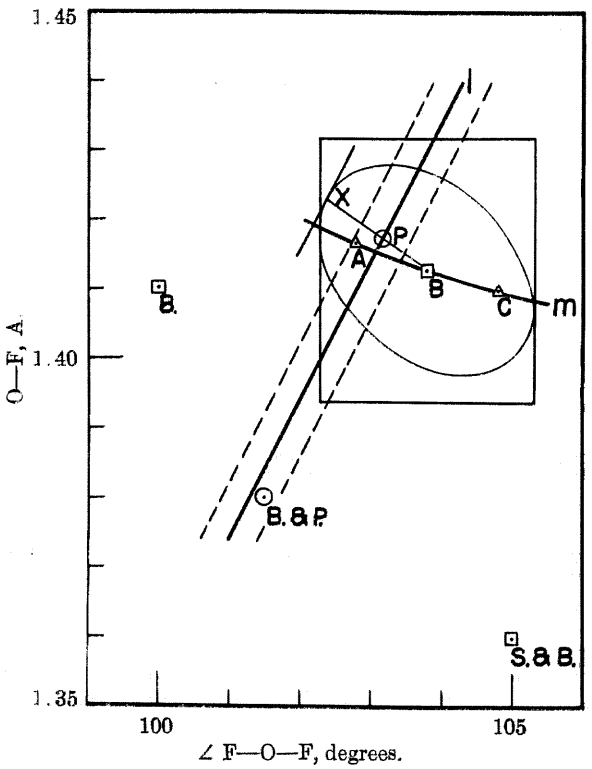

Fig. 2.—Bond length and bond angle values for OF_2. See text and Table II.

the positions read from curves A, B and C, with the results shown on curve m of Fig. 2. The details of the comparison are given for curve B by Table I.

In regard to Table I, some special remarks are in order. We give the unbiased estimate $s = \{\Sigma w_i(x_i - \bar{x})^2/(n-1)\}^{1/2}$ of the standard deviation of a $(q_{calc.}/q_{obs.})_i = x_i$ value of unit weight, as well as the weighted average deviation $\Sigma w_i|x_i - \bar{x}|/\Sigma w_i$, which, although quoted in our previous papers, seems to have no simple statistical meaning if the weights are not all equal.

Two related points confirm the belief, commonly held in this work, that truly random errors in the measurements of ring diameters are unimportant: the estimated standard deviation of the weighted mean $s/(\Sigma w_i)^{1/2}$ is about ±0.0015, considerably less than would correspond to the limit of error ±1.0% which, in accordance with our experience, had to be assigned to the scale factor; and even the deviations $(x_i - \bar{x})$ appear to represent mainly systematic error, since the four to thirteen individual measurements per ring by each observer lead to estimates of the standard deviations of the x_i that amount typically to only about a third of the values which correspond to s and the w_i as given in Table I.

TABLE I

ELECTRON DIFFRACTION DATA FOR OF_2

Min.	Max.	$q_{obs.}$	$q_B/q_{obs.}$	Wt. (w_i)
1		8.43	1.091	0
	1	11.71	1.016	0
2		14.79	0.960	0
	2	18.85	0.987	2
3		24.67	0.997	5
	3	30.09	1.017	0
4		33.32	1.035	0
	4	36.59	1.017	0
5		41.30	0.964	0
	5	46.44	0.997	10
6		52.23	0.998	10
	6	58.12	1.007	0
7		59.65	1.018	0
	7	62.20	1.013	0
8		67.94	0.999	10
	8	74.73	0.989	10
9		81.43	0.980	1
	9	89.51	0.993	1
10		96.59	0.990	2
Weighted mean:				0.9949
Estimated standard deviation of value of unit weight (s):				0.012
Weighted average deviation:				0.004

The weights were first assigned in about the usual way, *i.e.*, a smooth function of q rising from zero for the inner rings and falling toward zero again for the outermost rings was modified by factors of a half or a quarter for minor or for highly unsymmetrical features. The distribution of the resulting quantities $w_i(x_i - \bar{x})^2$ with respect to q and to classes of features—maxima *vs.* minima, the symmetrical *vs.* the unsymmetrical, etc.,—was satisfactory except that the weights for the unsymmetrical features (max. 1, 3, 4, 6, 7; min. 1, 2, 4, 5, 7) needed to be reduced by a factor of about one-tenth in order to equalize the estimates s to be obtained separately from them and from the symmetrical features. The final weights (Table I) were placed on a scale of ten and so vanish for all unsymmetrical features. This is satisfactory for the calculation of the average, but is hardly satisfactory for the estimation of the standard deviation. With this reservation, however, zero weights are indicated in most cases, as in reference 10, where fractional weights have been used for complex features. The above argument applies to the averaging of measurements by J. I. and V. S., but we have used only the simple averages.

We would emphasize that these remarks, despite their stress on other details are not intended to detract from the usual scrutiny of the $(q_{calc.}/q_{obs.})$ values for possible trends or for undue sensitivity of the average to reasonable variations of the weights. In this regard, the present average is somewhat more sensitive than usual.

The results from this and from previous electron diffraction investigations are given in the first three lines of Table II. The fourth entry represents Bernstein and Powling's adjustment of Boersch's result to the region between the dashed

TABLE II

THE STRUCTURE OF OF_2

O—F, Å.	∠ F-O-F, degrees	
1.36 ± 0.1	105 ± 5	Sutton and Brockway[7]
1.41 ± 0.05	100 ± 3	Boersch[8]
1.413 ± 0.019	103.8 ± 1.5	Present work
1.38 ± 0.03	101.5 ± 1.5	Bernstein and Powling[2]
1.418	103.2	Best value

(7) L. E. Sutton and L. O. Brockway, *J. Am. Chem. Soc.*, **57**, 473 (1935).

(8) H. Boersch, *Monatsh.*, **65**, 311 (1935)

lines in Fig. 2 defined for a rigid model by their value 1.60 ± 0.02 cm.$^{-1}$ for the rotational constant $A'' - B''$, and the last entry represents our related adjustment of the present result.

Our adjustment (see Fig. 2) differs from Bernstein and Powling's in that we take the point P lying on the line l defined by $A'' - B'' = 1.60$ cm.$^{-1}$ which seems most probable on the basis of the electron diffraction work. For this purpose we have assumed a probable error function which depends upon a sum of the squares of the errors in bond angle and in the scale factor, with coefficients such that the limiting errors in bond angle (±1.5°) and in the scale factor (±1.0%) correspond to the same probability. Plotted as a function of bond angle and bond length with the help of the linear relation between assumed bond angle and resultant bond length which is approximated at B by curve m, the corresponding ellipse takes the form shown; the indicated construction for P follows. (It is appropriate to place P exactly on l, since the indicated relative weights of the spectroscopic and diffraction data for the location of P along the line BX are about 20:1.) For their adjustment, on the other hand, Bernstein and Powling essentially used their result to reduce Boersch's limits of error and quoted only rounded values for a point symmetrically located with respect to the reduced limits.

It is notable that in OF_2 the bond angle is greater than in NF_3 (102°9',[9] 102.5° [10]), whereas in H_2O (105°3' [11]) it is less than in NH_3 (106°47'[11]). Nevertheless, the bond angle in OF_2 is somewhat less than in H_2O, in agreement with a discussion previously given for NF_3 and NH_3.[10] The new O—F bond length, being appreciably greater than Bernstein and Powling's value, is again in good agreement with the radius values and interpolation formula given previously.[12]

(9) J. Sheridan and W. Gordy, *Phys. Rev.*, **79**, 513 (1950).

(10) V. Schomaker and C. S. Lu, *J. Am. Chem. Soc.*, **72**, 1182 (1950).

(11) G. Herzberg, "Infrared and Raman Spectra of Polyatomic Molecules," D. Van Nostrand Co., Inc., New York, N. Y., 1945, pp. 489, 439.

(12) V. Schomaker and D. P. Stevenson, *J. Am. Chem. Soc.*, **63**, 37 (1941).

Part II

The Failure of the Born Approximation --- The Calculation of Complex Atomic Scattering Amplitudes for Electron Diffraction

A.

If it is assumed that the molecular scattering amplitude is simply a superposition of atomic scattering amplitudes, the intensity of coherent scattering of a beam of electrons at angle θ by randomly oriented molecules is

$$I(s) = c \sum_{i,j} \left|f_i(\theta)\right| \left|f_j(\theta)\right| \cos\left\{\eta_i(\theta) - \eta_j(\theta)\right\} \frac{\sin sr_{ij}}{sr_{ij}} \qquad (1)$$

where c is a constant, r_{ij} is the distance between atoms i and j in the molecule, $f_j(\theta) = \left|f_j(\theta)\right| e^{i\eta_j(\theta)}$ is the complex scattering amplitude for electrons of the jth atom, and s is $4\pi\lambda^{-1} \sin(\theta/2)$. The complex electron scattering amplitude $f(\theta)$ is evaluated by solving the problem of the elastic scattering of electrons by a central potential $V(r)$*, where $V(r)$ is the potential energy of the incident electron in the atomic field. This amounts to seeking solutions of the Schrödinger equation**

$$\nabla^2\psi + (k^2 - U(r))\psi = 0 \qquad (2)$$

where

$$k = 2\pi/\lambda, \qquad U(r) = (-2k\alpha/Ze^2)\, V(r), \qquad \alpha = -Ze^2/\hbar v$$

The wave function ψ must at large distances from the nucleus

---

* For a general reference, see (1).
** For simplicity, the non-relativistic equation is written.

represent both the incident plane wave and a scattered spherical wave:

$$\psi \sim e^{ikz} + e^{ikr}\, r^{-1}\, f(\theta) \tag{3}$$

with θ measured relative to the z axis. A general solution of equation (2) having axial symmetry is

$$\psi = \sum_{l=0}^{\infty} A_l\, P_l(\cos\theta)\, T_l(r) \tag{4}$$

where the A_l are arbitrary constants and T_l is any solution of

$$\frac{1}{r^2}\frac{d}{dr}\left(r^2\frac{dT}{dr}\right) + \left(k^2 - U(r) - \frac{(l)(l+1)}{r^2}\right) T = 0. \tag{5}$$

The wave function ψ must be everywhere finite; therefore, T_l must be chosen to be that solution of equation (5) which is finite at the origin. The particular solution which is finite at the origin can be shown to have the form

$$C\, r^{-1} \sin(kr - \pi l/2 + \delta_l)$$

where C is an arbitrary constant and the phase δ_l is a constant which depends on k and on $U(r)$. To fix C, $T_l(r)$ is defined as the bounded solution of equation (5) which has the asymptotic form

$$T_l(r) \sim (kr)^{-1} \sin(kr - \pi l/2 + \delta_l). \tag{6}$$

The A_ℓ are chosen so that equation (4) will have the asymptotic form required by equation (3), and it is found that

$$A_\ell = (2\ell+1)\, i^\ell\, e^{i\delta_\ell}\,.$$

Equation (4) which describes the incident and scattered waves then becomes

$$\psi = \sum_{\ell=0}^{\infty} (2\ell+1)\, i^\ell\, e^{i\delta_\ell}\, T_\ell(r)\, P_\ell(\cos\theta),$$

and the asymptotic form of the scattered wave is $e^{ikr}\, r^{-1}\, f(\theta)$ with

$$f(\theta) = (2ik)^{-1} \sum_{\ell=0}^{\infty} (2\ell+1)\, (e^{2i\delta_\ell} - 1)\, P_\ell(\cos\theta). \qquad (7)$$

Equation (7) is generally called the partial waves solution for $f(\theta)$.

The phases δ_ℓ may be obtained by numerical integration of equation (5). Other ways of determining the phases may be more convenient. If δ_ℓ is small, the formula

$$\delta_\ell^{\,o} = \frac{k\alpha\pi}{Ze^2} \int_0^\infty V(r)\, J^2_{\ell+\frac{1}{2}}(kr)\, r\, dr \qquad (8)$$

is useful. Also, the term $(e^{2i\delta_\ell} - 1)$ in equation (7) may be replaced by $(2i\,\delta_\ell)$; substitution of equation (8) for δ_ℓ then

yields the Born formula for $f(\theta)$*:

$$f^B(\theta) = \frac{2k\alpha}{Ze^2} \int_0^\infty V(r) \frac{\sin sr}{sr} r^2 \, dr. \tag{9}$$

The Born formula was originally obtained in the following way (2): It can be shown that equation (2) leads to

$$\psi \sim e^{ikz} - \frac{e^{ikr}}{4\pi r} \int U(r') \, e^{-ik \underline{n}\cdot\underline{r}'} \, \psi(\underline{r}') \, d\tau' \tag{10}$$

where $\underline{n}$ is a unit vector in the direction of $\underline{r}$. If it is assumed that the wave is not much diffracted by the scattering center, the perturbed wave $\psi(\underline{r}')$ in equation (10) may be replaced by the unperturbed wave $e^{ikz'}$. Use of equation (3) then yields $f^B(\theta)$ (equation (9)).

If δ_l is not small, the WKB method may be used to obtain

$$\delta_l = \int_{r_1}^\infty \left\{k^2 - U(r) - \left(\frac{l+\frac{1}{2}}{r}\right)^2\right\}^{\frac{1}{2}} dr - \int_{r_2}^\infty \left\{k^2 - \left(\frac{l+\frac{1}{2}}{r}\right)^2\right\}^{\frac{1}{2}} dr \tag{11}$$

where $r_1, r_2 > 0$ are the zeros of the respective integrands.**

---

* Use is made of the formula

$$\frac{\sin sr}{sr} = \frac{\pi}{2kr} \sum_{l=0}^\infty (2l+1) \, J^2_{l+\frac{1}{2}}(kr) \, P_l(\cos\theta).$$

** In equation (11), $(l)(l+1)$ has been replaced by $(l+\frac{1}{2})^2$ in accordance with the work of Langer (3).

The use of $f^B(\theta)$ or even of Z^* in the intensity formula proved adequate for many years. Some anomalous results for heavy-atom molecules were obtained, however. Uranium hexafluoride, for example, was found by Braune and Pinnow (4) in 1937 to be asymmetric with two short (1.78 Å), two intermediate (1.99 Å), and two long (2.17 Å) U-F distances. At that time there was little physical evidence to suggest that this structure was incorrect. Subsequently, dipole moment measurements and spectroscopic results strongly indicated that uranium hexafluoride was octahedral. Yet, Bauer's (5) wartime electron diffraction reinvestigation indicated that uranium hexafluoride was asymmetric, with three short (1.87 Å) and three long (2.17 Å) U-F distances.

Some workers (6) in the field of electron diffraction believed that such anomalous structures were indeed asymmetric and that the other physical measurements which pointed toward symmetric structures needed reinterpretation or redetermination. This faith in the theory, in the Born approximation, may be understood when it is remembered that for fifteen years electron

---

* The Born amplitude $f^B(\theta)$ is related to the atomic number Z by the formula

$$f^B(\theta) = (2ke^2/\hbar vs^2)(Z - F(\theta)) \qquad (12)$$

where $F(\theta)$ is the x-ray form factor. Only limited relative intensity data and no absolute intensity data are obtained from the visual interpretation of electron diffraction photographs (the visual method). Thus, $f^B(\theta)$ in equation (1) is usually replaced by Z with no effect on the final results.

diffraction data on gases had, in the hands of careful investigators, led to structures, except for those few anomalous ones, which were reasonable structurally and which were in essential agreement with the available data from other physical methods. Other workers suspected the Born approximation, but did not understand how a failure of the approximation would result in asymmetric structures.

Recently, Schomaker and Glauber (7,8) pointed out that if the Born approximation failed, thus if the scattering amplitudes were complex, the term $\cos(\eta_i(\theta) - \eta_j(\theta)) = \cos\Delta\eta_{ij}(\theta)$ would be introduced into equation (1) and the anomalous structures could be explained. If the amplitudes are real, a pair of split distances $r_{ij} = r_o - \Delta r$ and $r'_{ij} = r_o + \Delta r$ contribute to equation (1) as

$$f_i(\theta)\, f_j(\theta) \left\{ \frac{\sin sr_{ij}}{sr_{ij}} + \frac{\sin sr'_{ij}}{sr'_{ij}} \right\} \simeq 2\, f_i(\theta)\, f_j(\theta) \cos(s\Delta r)\, \frac{\sin sr_o}{sr_o} \qquad (13)$$

for $\Delta r/r_o$ small, and this is just the result one obtains with complex amplitudes and a symmetric structure ($r_{ij} = r'_{ij} = r_o$), if $\Delta\eta_{ij}$ is proportional to s. The electron diffraction pattern which with the Born approximation leads to an asymmetric structure may thus be expected to lead with complex amplitudes to a symmetric structure. Schomaker and Glauber carried out a treatment equivalent to the second Born approximation,* and with the assumptions that

---

* The second Born approximation may be thought of as the substitution of the result ψ^B of the first Born approximation for $\psi(\underline{r}')$ in equation (10).

the potential is screened-coulomb ($V(r) = -(Ze^2/r)\, e^{-r/a}$) and that $|f(\theta)|$ is given by $f^B(\theta)$, they obtained η/α as a function of $\ell = as$, where a is the screening radius defined by the relation*

$$a = a_o/Z^{1/3} \qquad (14)$$

From the arguments η of the complex scattering amplitudes Schomaker and Glauber calculated the splits in the absence of any actual distance splits and found remarkable agreement with the distance splits which had been obtained from observed diffraction patterns using the Born approximation. The arguments increase with increasing Z. The term $\Delta\eta_{ij}$ is larger therefore for a heavy-atom light-atom interaction and is more likely to take on the critical value $\pi/2$** within the observed s range. This explains why anomalous results were obtained only for those molecules which contained both a heavy atom and light atoms.

A short time later, Dr. Glauber (9) proposed a more refined treatment of the scattering problem which gives the argument and the

---

* In the work of Schomaker and Glauber and in the work described in Section B the factor 0.885 which usually appears in the numerator of the right-hand side of equation (14) is omitted. This omission, of course, does not affect the final results or the conclusions.

** The intensity is highly sensitive to the term $\Delta\eta_{ij}$ only when $\Delta\eta_{ij} = (2m+1)\pi/2$. The intensity is relatively insensitive to the lack of proportionality of $\Delta\eta_{ij}$ to s at other angles, and to the deviation of $|f(\theta)|$ from $f^B(\theta)$. These latter two effects could easily remain unnoticed, since accurate intensity measurements are not usually obtained in gas diffraction work.

magnitude of the scattered wave. Dr. Glauber obtains

$$f(\Theta) = (k/i) \int_0^\infty J_0(2kp \sin(\Theta/2))(e^{iX(p)} - 1)\, p\, dp \qquad (15)$$

where

$$X(p) = -(1/\hbar v) \int_{-\infty}^{\infty} V(\sqrt{y^2+p^2})\, dp. \qquad (16)$$

(Molière (10) obtains from equation (7) a form very similar to equation (15) by use of the Euler summation formula and the relation

$$P_l(\cos\Theta) \sim (\Theta/\sin\Theta)^{\frac{1}{2}} J_0\{(l+\tfrac{1}{2})\Theta\}\ .)$$

If the screened-coulomb field is assumed in equation (16), equation (15) becomes

$$f(\Theta)/ka^2 = i^{-1} \int_0^\infty J_0(lx)(e^{-2\alpha i K_0(x)} - 1)\, x\, dx. \qquad (17)$$

The quantities $\eta(\Theta)$ and $|f(\Theta)|$ were obtained as functions of α and of $l = as$ by numerical integration* of equation (17).

From equation (1) it can be seen that if the amplitudes are real, the intensity is a simple function of the wavelength, a change in wavelength merely results in a change in scale; if the amplitudes are complex, the intensity is a more complicated function of the wavelength. To test Dr. Glauber's treatment of the scattering problem and also to test Schomaker and Glauber's second Born calculation, it was therefore desirable to obtain reliable

---

* This numerical integration was done in collaboration with Mr. Gary Felsenfeld.

experimental data on the same compound at two different voltages. Electron diffraction photographs of uranium hexafluoride were obtained at 11 kev as well as at the usual 40 kev. Besides the change in scale, the patterns showed marked differences. This is the first direct experimental evidence for the failure of the Born approximation in electron diffraction.

A symmetric model was assumed for uranium hexafluoride, and the intensity was computed from equation (1). The arguments η of the second Born approximation led to a 40 kev intensity which was in satisfactory agreement with the photographs, but to an 11 kev intensity which was in serious disagreement with the photographs. The magnitudes and arguments of Dr. Glauber's treatment led to an intensity at either voltage which was in disagreement with the photographs.

The procedures used to obtain the uranium hexafluoride photographs, to test the second Born calculation, to evaluate numerically the necessary integral (equation (17)), and to test Dr. Glauber's treatment are described fully in Section B.

At this point there was no treatment which adequately explained the experimental facts. But finally, a more exact calculation was made in collaboration with Dr. Jean Hoerni. The partial waves solution was used (equation (7)), the phases were determined from the WKB method (equation (11)); the Thomas-Fermi potential was

adopted for uranium, the Hartree-Fock potential for fluorine. On the assumption that uranium hexafluoride is symmetric, excellent agreement has been found between the calculated intensities and the 40 kev and 11 kev visual data. The calculations have therefore been extended to other atoms at 40 kev. This work is described fully in Section C.

It may be said in conclusion that, as Schomaker and Glauber pointed out, the anomalous structures found by electron diffraction for heavy-atom molecules are explained by the failure of the Born approximation. This approximation has necessarily given way to a more involved calculation. Initial experimental evidence points to the adequacy of the new calculations, but a positive verification is not possible until more complete intensity data on a number of heavy-atom molecules are available.

B.*

Bromine-contaminated uranium hexafluoride, prepared by the action of bromine trifluoride on uranium metal, was kindly supplied by the Atomic Energy Research Department of North American Aviation, Inc., Downey, California. Resublimation of the uranium hexafluoride at reduced pressures removed most of the bromine. The purified compound gave the expected 40 kev electron diffraction pattern (4,5,11). Slight modification of the electron diffraction apparatus, in particular of the power supply and the filament geometry, was necessary in order to obtain 11 kev photographs of uranium hexafluoride. (The "40 kev" voltage was actually 39.47 kev by calibration with zinc oxide; the "11 kev" voltage was 11.38 kev from the value 39.47 and the potentiometer readings at both voltages.) Unfortunately, the sample bulb was found to contain a non-volatile residue when an attempt was made to obtain confirmative photographs at 40 kev. The assumption has been made that the photographs at 11 kev are actually of uranium hexafluoride. This assumption is surely justified by the facts that the pattern is too complex to be due to hydrogen fluoride, bromine, or other possible contaminants, and that there are very few volatile compounds of uranium.

---

* The work described in this section was done in collaboration with Mr. Gary Felsenfeld.

The 11 kev pattern differs markedly from the 40 kev pattern --- this is the first direct experimental evidence for the failure of the Born approximation in electron diffraction studies of gases.

Equation (1) may be modified for use with visual data and a symmetric uranium hexafluoride model to give

$$I(s)\,K(s) = \frac{6}{r_{U-F}} \cos\Delta\eta_{UF} \sin r_{U-F}s + \left|\frac{f_F}{f_U}\right| \left\{ \frac{12}{r_{F-F}} e^{-(a_{F-F} - a_{U-F})s^2} \sin r_{F-F}s + \frac{3}{r_{F.F}} e^{-(a_{F.F} - a_{U-F})s^2} \sin r_{F.F}s \right\} \qquad (18)$$

where $I(s)$ is the intensity of scattering, $K(s)$ is a smoothly decreasing function of s, and $e^{-a_{ij}s^2}$ is the temperature factor for the distance r_{ij} between atoms i and j.

For agreement between the intensity calculated for a symmetric model from complex amplitudes and the intensity calculated for an asymmetric model from the Born approximation (and thus for agreement with the visual data), it is essential that s_o, the point where $\Delta\eta_{ij}$ is $\pi/2$ be very close to s_b, the point where Δrs (equation (13)) is $\pi/2$. The modified intensity function $I(s)\,K(s)$ has been calculated for a symmetric model* of uranium hexafluoride

---

* $r_{U-F} = 2.00$ Å, $r_{F-F} = 2.83$ Å, $r_{F.F} = 4.00$ Å, $a_{F-F} - a_{U-F} = 2.2\ 10^{-3}$ Å^2, $a_{F.F} - a_{U-F} = 0.75\ 10^{-3}$ Å^2.

at 40 kev and at 11 kev from the η of the second Born calculation. At 40 kev, s_0 is 11.2 and s_b is about 10.5 (5) to 11.2 (11), and there is good agreement between the calculated intensity and the visual data. At 11 kev, s_0 is 3.8 and s_b is about 6.4 to 6.6, and agreement is not obtained.

The 40 kev and 11 kev data were used, however, to modify the plot of η/α vs. ℓ in an attempt to obtain agreement with experiment. An equation of the form

$$\cos \Delta\eta_{ij} = A + B \cos Cs \qquad (19)$$

was applicable over the entire s range at 40 kev (with A = -0.15, B = 0.85, and C = 0.125), and it was assumed that this form was also applicable at 11 kev. A radial distribution function (12) was computed from the visual data, and from the observed split the value of C was obtained. The radial distribution function also gave an approximate ratio of A to B. These values were then refined by the comparison of calculated curves with the visual curve. The best agreement with the visual curve was obtained with the values A = -0.02, B = 0.99, C = 0.235. Equation (19) was then used to revise the plot of η/α vs. ℓ of Schomaker and Glauber. Only a narrow low-ℓ range of the plot was modified by this procedure and the intensity function at 40 kev was hardly affected. Thus, the revision resulted in agreement of the calculated intensity with the data at both 40 kev and 11 kev.

It is doubtful, of course, whether this revised plot would be satisfactory for other heavy-atom molecules.

Attention was now turned to Dr. Glauber's new treatment which may be written

$$f(\theta)/ka^2 = i^{-1} \int_o^\infty J_o(\ell x)(e^{-2\alpha i K_o(x)} - 1)\, x\, dx, \qquad (17)$$

if the screened-coulomb field is assumed. Evaluation of the real (R) and the imaginary (I) parts of this integral lead to η and $|f(\theta)|$:

$$\eta = \tan^{-1} \frac{I}{R}, \qquad |f(\theta)| = (I^2 + R^2)^{\frac{1}{2}}.$$

R and I were evaluated with the help of a desk calculator from Simpson's rule for the following values of the parameters:

$$-\alpha = \tfrac{1}{2},\ 1,\ 2,\ 3; \quad \ell = 0,\ 1,\ 3,\ 6.$$

These values and the corresponding arguments are given in Table I.

Plots of η vs. ℓ for the desired α were obtained by interpolation on plots of η vs. α for constant ℓ. From these data the quantities s_o could be computed and compared with s_b. The screening radius for fluorine was assumed to be $a_o/Z^{1/3}$ (equation (14)) at both voltages, and no screening radius, independent of wavelength, could be found for uranium which would give the proper values of s_o. It also proved inadequate to equate the screening radius to $\gamma a_o/Z^{1/3}$, where γ is a

Table I

Numerical Integration of Equation (17)

ℓ	$-\alpha$	R	I	η
0	$\frac{1}{2}$	0.951	0.214	0.222
	1	1.563	0.629	0.383
	2	2.338	1.405	0.541
	3	2.814	2.039	0.627
1	$\frac{1}{2}$	0.424	0.181	0.403
	1	0.594	0.500	0.700
	2	0.535	0.970	1.067
	3	0.318	1.230	1.318
3	$\frac{1}{2}$	0.045	0.080	1.060
	1	- 0.055	0.145	1.933
	2	- 0.227	- 0.008	3.178
	3	- 0.186	- 0.204	3.972
6	$\frac{1}{2}$	- 0.004	0.025	1.711
	1	- 0.049	0.001	3.128
	2	0.036	- 0.070	5.193
	3	0.094	0.034	6.634

constant independent of both wavelength and atomic number.

Data are available on the apparent splits in several heavy-atom molecules at 40 kev (7). It was assumed that s_b was equal to s_o so that the data would permit the calculation of s_o. The screening radius a was assumed to be given by

$$a = \beta(Z, \lambda)\, a_o/Z^{1/3}. \tag{20}$$

The quantities $\beta(Z)$ were determined by successive approximation from the 40 kev s_o's. A smooth curve was drawn through these and through $\beta_H = 0.885$, the calculation was reversed, and the splits shown in Table II were obtained. The smoothed values $\beta_U = 1.63$ and $\beta_F = 0.925$ and the corresponding $|f(\theta)|$ gave a calculated intensity function which is in good agreement with the 40 kev visual data. The best agreement with the low voltage data, on the assumption that β_F is a weak function of the wavelength, is obtained with $\beta_F = 0.94$ and $\beta_U = 1.93$. Data obtained at 11 kev for other molecules would be needed to define further the relation of β to Z at that voltage.

Tables III and IV present observed ring-diameter positions in units of $q = 10\, s/\pi$ for 40 kev and 11 kev uranium hexafluoride together with positions obtained from the various calculations just described. A comparison of $q_{calc.}$ with $q_{obs.}$ does indicate to some extent the adequacy of the calculated intensity function, particularly if there is good

Table II

Apparent Distance Splits --- 40 kev

Substance	Distance	Apparent Splits, Å			
		Obs.[a]	Calc.[a] (V.S. & R.G.)	Calc.[b] (Glauber)	Calc.[c] (J.H. & J.I.)
UF_6	U-F	0.30, 0.28	0.28	0.31	0.27
OsO_4	Os-O	0.23	0.24	0.25	0.24
WF_6	W-F	0.23	0.22	0.23	0.23
$W(CO)_6$	W-C	0.24	0.24	0.25	0.25
$W(CO)_6$	W-O	0.23	0.23	0.24	0.24
WCl_6	W-Cl	~0.18	0.18	0.20	0.18
IF_5	I-F	0.18	0.15	0.16	0.17
MoF_6	Mo-F	0.14	0.12	0.12	0.12
$Mo(CO)_6$	Mo-C	0.13	0.13	0.14	0.15
$Mo(CO)_6$	Mo-O	0.13	0.12	0.13	0.13

---

a See reference (7).
b The following values of β were used: U = 1.63, F = 0.925, Os = 1.41, O = 0.92, W = 1.39, C = 0.91, Cl = 0.97, I = 1.21, Mo = 1.12.
c See Section C.

Table III

40 kev Uranium Hexafluoride Data

Min.	Max.	$q_{obs.}$[a]	$q_{calc.}/q_{obs.}$			Weight
			Bauer[b]	2nd Born	Glauber[c]	
1		6.6				0
	1	11.0	1.061		1.045	0
2		18.6	0.962	0.989	0.978	4
	2	22.6	0.991	0.991	1.000	6
3		26.5	1.023	1.019	1.015	2
	3	30.5	1.013	1.007	1.003	3
4		34.0	0.976	1.000	0.982	3
	4	37.5	0.987	0.987	0.997	4
5		42.4	0.991	0.993	0.995	8
	5	47.5	0.985	0.998	0.992	6
6		53.2	0.983	0.985	0.998	9
	6	58.0	0.984	1.000	0.995	10
7		63.3	0.979	0.987	0.986	10
	7	67.8	0.982	0.999	0.988	10
8		72.6	0.993	0.996	1.001	9
	8	77.9	0.983	0.997	0.996	8
9		82.3	0.994	1.002	1.002	6
	9	86.9	0.992	1.006	1.003	4
10		92.0	0.992	1.007	1.003	2
	10	96.6	0.995	1.007	1.007	0
Weighted mean:			0.9866	0.9957	0.9950	
Estimated standard deviation of value of unit weight[d]:			0.025	0.018	0.018	($\Sigma W = 104$)

---

a These data are from the visual curve of Dr. O. Bastiansen (11). Bauer (5) did not define his wavelength clearly so his visual data were not used.

b These were obtained from Bauer's "Best Model", model A_4.

c These were calculated from equation (17), using the adjusted screening radii.

d See reference (13).

Table IV

11 kev Uranium Hexafluoride Data

Min.	Max.	$q_{obs.}$[a]	$q_{calc.}/q_{obs.}$		Weight
			2nd Born[b]	Glauber[c]	
1		6.7	0.950	0.964	0
	1	11.0	0.998	0.989	1
2		13.3	0.983	0.983	5
	2	15.6	0.974	0.987	3
3		19.2	0.989	0.989	10
	3	22.5	1.001	0.988	2
4		25.7	1.006	0.975	3
	4	29.6	0.987	0.974	4
5		33.2	0.997	0.994	7
	5	37.3	0.997	0.997	10
6		42.2	0.995	0.997	7
	6	47.0	1.000	1.000	5
7		53.6		0.995	1
Weighted mean:			0.9931	0.9900	
Estimated standard deviation of value of unit weight[d]:			0.018	0.018	($\Sigma W = 58$)

---

a These are observations of J. Ibers.
b These were calculated from the revised plot of η/α vs. ℓ .
c These were calculated from equation (17), using the adjusted screening radii.
d See reference (13).

agreement near the critical region of the curve ($q_b = 10\ s_b/\pi$ is about 34.5 at 40 kev and about 20.6 at 11 kev). Agreement between the calculated curve and the data cannot be claimed, however, on this basis alone; more important, it is essential that a detailed feature-by-feature comparison of the calculated curve with the visual curve show satisfactory agreement.

It is true that with suitably adjusted screening radii Dr. Glauber's treatment of the scattering problem has led to agreement with the limited experimental data. It may be argued that the introduction of such screening radii is less arbitrary than the correction which was applied to the second Born calculation, but surely it is difficult to find a physical basis for wavelength-dependent screening radii. It is important to point out, moreover, that the assumption that atomic potentials are screened-coulomb is extremely difficult to justify, and that the success of the second Born calculation at 40 kev might well be fortuitous. The failure of the second Born calculation at 11 kev and of Dr. Glauber's treatment at both 40 kev and 11 kev demands the use of more realistic atomic potentials; the arbitrary modification of the second Born calculation or of the screening radii is hardly justified.

References

Sections A and B

(1) N. F. Mott and H. S. W. Massey, "The Theory of Atomic Collisions," (Oxford University Press, London, 1949), second edition, particularly Chapters II and VII.

(2) M. Born, Z. Physik 38, 803 (1926).

(3) R. E. Langer, Bull. Am. Math. Soc. 40, 574 (1934); Phys. Rev. 51, 669 (1937).

(4) H. Braune and P. Pinnow, Z. phys. Chem. B35, 239 (1937).

(5) S. Bauer, J. Chem. Phys. 18, 27 (1950).

(6) For example, S. Bauer, J. Phys. Chem. 56, 343 (1952).

(7) V. Schomaker and R. Glauber, Nature 170, 290 (1952).

(8) R. Glauber and V. Schomaker, Phys. Rev. 89, 667 (1953).

(9) R. Glauber, private communication (1952).

(10) G. Molière, Z. Naturforsch. 2a, 142 (1947).

(11) O. Bastiansen, unpublished work in these laboratories.

(12) P. A. Shaffer, Jr., V. Schomaker, and L. Pauling, J. Chem. Phys. 14, 659 (1946).

(13) J. A. Ibers and V. Schomaker, J. Phys. Chem. 57, 699 (1953).

C.

Dr. Glauber left no detailed derivation of his formulas nor an indication of the relation of his results to others in the literature when he returned to Harvard University. (Molière's paper suggests that one could obtain results very similar to Dr. Glauber's from the partial waves treatment.) As a result, the lack of understanding of Dr. Glauber's treatment persisted.

Dr. Jean Hoerni, therefore, made some preliminary calculations based on the partial waves treatment, with phases determined from the WKB method. The preliminary results were promising and more extensive calculations were carried out. These are described in the following two reprints. Attention is called to Table II of Section B where for comparison the apparent distance splits obtained in the calculations to be described are given.

Reprinted from THE PHYSICAL REVIEW, Vol. 91, No. 5, 1182-1185, September 1, 1953
Printed in U. S. A.

Complex Amplitudes for Electron Scattering by Atoms*

JEAN A. HOERNI AND JAMES A. IBERS†
Gates and Crellin Laboratories of Chemistry, California Institute of Technology,‡ Pasadena, California
(Received May 26, 1953)

The partial waves scattering theory has been applied to electron scattering by U and F atoms at 40 and 11 kev. The electron scattering by the UF_6 molecule, predicted from these results, is in good agreement with experiment.

I. INTRODUCTION

RECENTLY, Schomaker and Glauber[1] have pointed out that anomalies, e.g., apparent asymmetry, in the structures of molecules containing both heavy and light atoms as determined by electron diffraction can be removed by using complex atomic scattering amplitudes $f(\theta)$ and hence by rejecting the first Born approximation which gives only real amplitudes. This approximation, although theoretically justified only for $-\alpha=Ze^2/(h\nu)$ small, has nevertheless been universally employed in investigations of the molecular structure of gases by electron diffraction. Using the second Born approximation, Glauber and Schomaker[2] evaluated the phase of the complex amplitude, $\eta(\theta)=\arg f(\theta)$, for the exponentially screened Coulomb potential $-Ze^2e^{-r/a}/r$; agreement was obtained for a large group of molecules at 40 kev. However, good agreement is not obtained for the UF_6 pattern at 11 kev,[3] and, in any case, the second Born approximation and the assumption of the screened Coulomb field are both uncertain, so that a more adequate calculation is desired. We describe below an application of the partial waves scattering theory to the problem of the scattering of electrons by atoms (U and F). The energies considered (11 and 40 kev) are sufficiently high so that electron exchange and polarization effects can be neglected.

II. THEORY[4]

The solution to the problem of the elastic scattering of a beam of particles by a central potential $V(r)$ is given by

$$f(\theta)=(2ik)^{-1}\sum_{l=0}^{\infty}(2l+1)(e^{2i\delta_l}-1)P_l(\cos\theta), \qquad (1)$$

where θ is the scattering angle, k is $2\pi/\lambda$, and the phases δ_l may be interpreted as the phase differences between the perturbed and unperturbed radial functions at large distances from the nucleus. The δ_l's can be evaluated in several ways for electron scattering. When $\delta_l\ll 1$, (1) can be rewritten as

$$f(\theta)=k^{-1}\sum_{l=0}^{\infty}(2l+1)\delta_l P_l(\cos\theta), \qquad (2)$$

and the δ_l's are given by

$$\delta_l^0=\frac{k\alpha\pi}{Ze^2}\int_0^{\infty}V(r)J_{l+\frac{1}{2}}^2(kr)rdr. \qquad (3)$$

Substitution of (3) into (2) yields the first Born approximation for the scattering amplitudes, namely,

$$f^B(\theta)=\frac{2k\alpha}{Ze^2}\int_0^{\infty}V(r)\frac{\sin(sr)}{sr}r^2dr, \qquad (4)$$

where $s=2k\sin(\theta/2)$. When the δ_l's are not small, they may be evaluated conveniently by the WKB method. Starting with the relativistic Schrödinger equation,

$$\nabla^2\psi+\kappa^2(r)\psi=0, \qquad (5)$$

where

$$\kappa^2(r)=\frac{[E-V(r)]^2-m^2c^4}{h^2c^2}=k^2+\frac{V^2(r)-2EV(r)}{h^2c^2},$$

we obtain

$$\delta_l=\int_{r_1}^{\infty}G(r)dr-\int_{r_2}^{\infty}G_0(r)dr, \qquad (6)$$

with

$$G(r)=\{\kappa^2(r)-[(l+\tfrac{1}{2})/r]^2\}^{\frac{1}{2}},\quad G_0(r)=\{k^2-[(l+\tfrac{1}{2})/r]^2\}^{\frac{1}{2}}.$$

Here, the energy E includes the rest energy, and r_1, $r_2>0$ are the zeros of the respective integrands. In accordance with the work of Langer,[5] we have replaced $l(l+1)$ by $(l+\frac{1}{2})^2$. The δ_l's may also be evaluated exactly. This has been done by Bartlett and Welton[6] with a differential analyzer for Hg at 100 and 230 kev starting with Gordon's solutions of the Dirac equation. Although the δ_l's from the WKB method are generally supposed to be reliable only when large, and hence only when l is small, Bartlett and Welton found these values to be in excellent agreement with the exact values over the entire range of l; they found the δ_l^0's to be reliable at large l.

* This work was supported in part by the U. S. Office of Naval Research.
† National Science Foundation Predoctoral Fellow, 1952-1953.
‡ Contribution No. 1812.
[1] V. Schomaker and R. Glauber, Nature **170**, 290 (1952).
[2] R. Glauber and V. Schomaker, Phys. Rev. **89**, 667 (1953).
[3] Preliminary results by G. Felsenfeld and J. Ibers.
[4] As a general reference, we give N. F. Mott and H. S. W. Massey, *The Theory of Atomic Collisions* (Oxford University Press, London, 1949), second edition, particularly Chapter VII.
[5] R. E. Langer, Bull. Am. Math. Soc. **40**, 574 (1934); Phys. Rev. **51**, 669 (1937).
[6] J. H. Bartlett, Jr., and T. A. Welton, Phys. Rev. **59**, 281 (1941).

III. PROCEDURE AND RESULTS

We first compute the complex atomic scattering amplitudes for U and F at 40 and 11 kev and then apply these to the scattering by the UF_6 molecule. UF_6 was selected because it offers the most severe test (the molecule exhibits the largest apparent asymmetry[1]) and because only for it do we have electron diffraction photographs prepared at 11 kev as well as at the usual 40 kev.

For U we adopted the Thomas-Fermi potential, using the approximate form[7]

$$V(r)=-\frac{Ze^2}{r}\sum_{i=1}^{3}a_i e^{-b_i r/a}, \tag{7}$$

where $a_1=0.10$, $a_2=0.55$, $a_3=0.35$, $b_1=6.0$, $b_2=1.2$, $b_3=0.3$, and a, the screening radius, is $0.4685/Z^{\frac{1}{3}}$. For F we used the Hartree potential[8] in the approximate form

$$V(r)=-(Ze^2/r)(e^{-\beta_1 r}+ce^{-\beta_2 r}), \tag{8}$$

where $\beta_1=3.94$, $\beta_2=17.0$, and $c=-2.67$. Preliminary calculations indicated that the effect of electron spin would be important only for $l\leqslant 2$,[9] and since in the final summation (1) these terms are reduced in importance by the factor $2l+1$, we felt justified in adopting the relativistic Schrödinger equation (5). For small l, the δ_l's were calculated for 40 and 11 kev from the WKB expression (6); for large l ($\geqslant 25$), it was found that the δ_l^0's (3) and δ_l's (6) were in excellent agreement, as anticipated from the work of Bartlett and Welton.[6] With the δ_l's obtained in this way (Table I), we have evaluated the magnitudes $|f(\theta)|$ and the arguments $\eta(\theta)$ of the complex scattering amplitudes (Table II). The δ_l's for U can also be computed over the entire l range from the asymptotic expression (15) below. In this case, although the δ_l's differ from the above by as much as 8 percent at 40 kev and 15 percent at 11 kev, the resultant magnitudes and arguments in no case differ by more than 3 percent from those in Table II, the relative error increasing with increasing θ.

In the application of these results to the molecule UF_6, the assumption is made that multiple scattering and valence distortion are negligible. Then for visual data the following expression for the intensity function (specialized for the case of UF_6) is suitable:

$$\begin{aligned}I(s)K(s)=&(6/r_{U-F})\cos[\eta_U(\theta)-\eta_F(\theta)]\sin(r_{U-F}s)\\&+(|f_F(\theta)|/|f_U(\theta)|)\\&\times\{(12/r_{F-F})\{\exp[-(a_{F-F}-a_{U-F})s^2]\}\sin(r_{F-F}s)\\&+(3/r_{F\cdot F})\{\exp[-(a_{F\cdot F}-a_{U-F})s^2]\}\sin(r_{F\cdot F}s)\},\end{aligned} \tag{9}$$

where $I(s)$ is the modified scattering intensity, $K(s)$ is is a smoothly decreasing function of s, and $\exp(-a_{ij}s^2)$ is the temperature factor for the distance r_{ij} between atoms i and j.[1,10] Using our complex amplitudes and a symmetric UF_6 model,[11] we have evaluated the function $I(s)K(s)$ at 11 and 40 kev. Figure 1 compares the calculated and the visually estimated versions of this function. When one considers that the visual curves are significant only for comparisons of intensity over a small range of s (e.g., that one usually can compare the height of maximum n only with the average of the heights of maximum $n+1$ and maximum $n-1$), the agreement is excellent. For the present purpose, the most significant parts of the patterns are the very sensitive regions where $\eta_U(\theta)-\eta_F(\theta)=\pi/2$, and these are reproduced satisfactorily (Table III).

TABLE I. Selected values of δ_l.[a]

l	Uranium 40 kev	Uranium 11 kev	Fluorine 40 kev	Fluorine 11 kev
0	6.11	7.20	0.571	1.05
2	3.49	4.67	0.414	0.555
4	2.47	2.96	0.317	0.391
6	1.87	2.06	0.258	0.297
8	1.53	1.52	0.218	0.234
10	1.26	1.16	0.189	0.188
15	0.847	0.679	0.135	0.113
20	0.602	0.441	0.101	0.071
25	0.452	0.302	0.077	0.046
30	0.353	0.212	0.059	0.029
35	0.282	0.152	0.046	0.019
40	0.228	0.110	0.036	
50	0.155	0.059	0.022	
70	0.076	0.018		
100	0.028			

[a] The actual values used were 39.470 and 11.380 kev.

Table II also provides a comparison with the magnitudes $f^B(\theta)$ calculated by the first Born approximation[12] [using (18) and (19)] and the phase angles $\eta^B(\theta)$ for U calculated by the second Born approximation. For the latter it was necessary to extend the calculations of Glauber and Schomaker[2] to the potential for U used here. Their formula is

$$\eta^B(\theta)=\eta^B(\mathbf{k}',\mathbf{k})=\frac{k}{4\pi f^B(\theta)}\times\int f^B(\mathbf{k}'\mathbf{k}'')f^B(\mathbf{k}'',\mathbf{k})d\Omega_{\mathbf{k}''}, \tag{10}$$

[7] G. Molière, Z. Naturforsch. 2a, 142 (1947).
[8] F. W. Brown, Phys. Rev. 44, 214 (1933).
[9] See reference 4, Chap. IV, Eq. (23).
[10] Shaffer, Schomaker, and Pauling, J. Chem. Phys. 14, 659 (1946).
[11] $r_{U-F}=2.00$A, $r_{F-F}=2.83$A, $r_{F\cdot F}=4.00$A, $a_{F-F}-a_{U-F}=2.2\times10^{-3}A^2$, $a_{F\cdot F}-a_{U-F}=0.75\times10^{-3}A^2$.
[12] It should be noted that $f^B(\theta)$ is related to $F(\theta)$, the x-ray form factor, by the relation

$$f^B(\theta)=(-2ka/s^2)[1-(F(\theta))/Z].$$

The $F(\theta)$ for U obtained from the corresponding $f^B(\theta)$ given in Table II agree to within 1½ percent with the Thomas-Fermi values given in *Internationale Tabellen zur Bestimmung von Kristallstrukturen* (Gebrüder Borntraeger, Berlin, 1935), Vol 2, p. 573. The $F(\theta)$ for F agree to within 10 percent with those of R. W. James and G. W. Brindley [Phil. Mag. 12, 81 (1931)], and to within 6 percent with the f of R. McWeeny [Acta Cryst. 4, 513 (1951)]; our values being in general lower than those of McWeeny and higher than those of James and Brindley. We suspect these differences arise from differences in the models used.

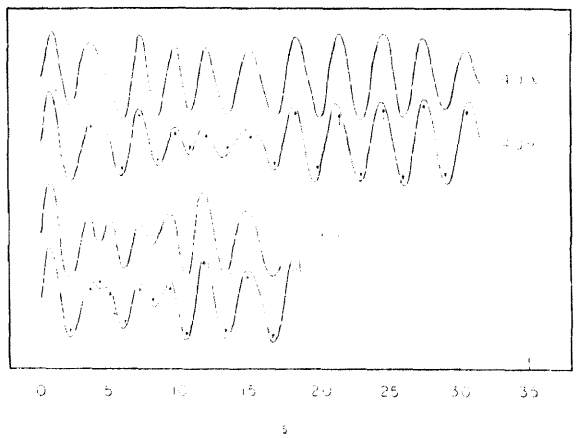

FIG. 1. Intensity curves for UF_6. "V" visual, "C" calculated for "40" or "11" kev. Further photographs will be made both at 40 and 11 kev, and the visual curves (40 V is due to Dr. Otto Bastiansen and 11 V to Felsenfeld and Ibers (reference 3)) are not to be regarded as final.

where $\mathbf{k}$ and $\mathbf{k}'$ refer to the directions of incidence and scattering, respectively, and $\mathbf{k}''$ is integrated over the sphere $|\mathbf{k}''|=k$. When the potential (7) for U was inserted and the integration performed there resulted

$$\eta^B(\theta)=\frac{\alpha^2}{2kf^B(\theta)\cos(\theta/2)}\sum_{i,j=1}^{3}\frac{a_ia_j}{\mu_{ij}}\times\tanh^{-1}\frac{2\mu_{ij}\cos(\theta/2)}{g_{ii}g_{jj}-\cos\theta}, \quad (11)$$

$$g_{ij}=1+(b_i^2+b_j^2)/(4k^2a^2),$$

$$\mu_{ij}=\{[(b_i^2-b_j^2)/(4k^2a^2)]^2+[g_{ij}^2-\cos^2(\theta/2)]\tan^2(\theta/2)\}^{\frac{1}{2}},$$

which is in serious disagreement with the partial waves values and with experiment, as may be seen from Tables II and III. The good agreement with experiment obtained previously[2] must be due to a fortuitous cancellation of errors: For heavy atoms the exponentially screened Coulomb field is quite unsatisfactory and (10), even at 40 kev, is inadequate.

It is planned to extend the calculations for 40-kev electrons to other atoms with the hope of achieving a sufficiently general theoretical basis for electron diffraction studies of the molecular structures of gases.

We thank Professor Verner Schomaker for reading this paper and for making many helpful suggestions.

IV. APPENDIX—MATHEMATICAL DETAILS

The Phases δ_l and δ_l^0

When computing δ_l it is convenient to split up (6) as follows:

$$\delta_l=\int_{r_1}^{r_3}G(r)dr-\int_{r_2}^{r_3}G_0(r)dr+\int_{r_3}^{\infty}[G(r)-G_0(r)]dr$$

$$=I_1-I_2+I_3. \quad (12)$$

Here, r_3 is sufficiently large so that for $r>r_3$, $G(r)$ and $G_0(r)$ do not differ by more than 10 percent. Then I_3 reduces to

$$I_3=\frac{k\alpha}{Ze^2}\int_{r_3}^{\infty}[V(r)]/[G_0(r)]dr. \quad (13)$$

r_1 was evaluated graphically and I_1 was integrated numerically using Simpson's rule; I_2 can be integrated analytically. I_3(13) can be expressed in terms of various power expansions and when $V(r)$ is given by (7), the following expression is convenient:

$$I_3=-\alpha\sum_{i=1}^{3}a_i\int_{r_3}^{\infty}[e^{-b_ir/a}]/[r^2-((l+\tfrac{1}{2})/k)^2]^{\frac{1}{2}}dr,$$

$$=-\alpha\sum_{i=1}^{3}a_i\left\{K_0(u_i)-e^{-u_i}\left[m-u_i\frac{m^3}{3!}+(3u_i^2-u_i)\frac{m^5}{5!}-(15u_i^3+u_i-15u_i^2)\frac{m^7}{7!}+\cdots\right]\right\}, \quad (14)$$

$$u_i=b_i(l+\tfrac{1}{2})/(ka), \quad m=\cosh^{-1}[(r_3k)/(l+\tfrac{1}{2})].$$

For large values of l ($\gtrsim 25$), it was found that $r_1\approx r_2\approx r_3$,

TABLE II. Magnitudes and arguments of the scattering amplitudes.

	Uranium								Fluorine					
	40 kev				11 kev				40 kev			11 kev		
θ	$\lvert f(\theta)\rvert$	$\eta(\theta)$	$f^B(\theta)$	$\eta^B(\theta)$	$\lvert f(\theta)\rvert$	$\eta(\theta)$	$f^B(\theta)$	$\eta^B(\theta)$	$\lvert f(\theta)\rvert$	$\eta(\theta)$	$f^B(\theta)$	$\lvert f(\theta)\rvert$	$\eta(\theta)$	$f^B(\theta)$
0	14.51	0.317	17.24	0.50	12.01	0.414	16.36	0.90	2.31	0.079	2.32	2.15	0.141	2.20
1	10.30	0.424	12.78		10.64	0.456	14.88		1.90	0.093	1.91	2.03	0.148	2.08
2	5.54	0.687	7.52		7.85	0.579	11.78		1.24	0.128	1.24	1.73	0.169	1.77
3	3.21	1.00	4.74	1.39	5.37	0.772	8.86	1.51	0.776	0.179	0.781	1.39	0.201	1.43
4	2.08	1.31	3.27		3.67	1.01	6.72		0.507	0.231	0.511	1.08	0.243	1.12
5	1.46	1.60	2.42		2.61	1.28	5.23		0.349	0.281	0.352	0.841	0.290	0.871
6	1.08	1.88	1.87	2.41	1.94	1.57	4.18	2.63	0.252	0.329	0.254	0.660	0.341	0.685
7	0.837	2.16	1.49		1.52	1.85	3.44		0.190	0.376	0.192	0.525	0.396	0.546
8	0.683	2.42	1.21		1.24	2.13	2.88		0.148	0.420	0.149	0.424	0.447	0.442
10	0.500	2.89	0.848	3.44	0.930	2.64	2.12	3.96	0.096	0.487	0.098	0.291	0.552	0.302
12	0.403	3.26	0.624		0.756	3.03	1.63		0.068	0.551	0.070	0.211	0.651	0.218
14	0.327	3.61	0.478		0.623	3.34	1.30		0.051	0.623	0.052	0.162	0.748	0.164
16	0.263	3.95	0.378	4.64	0.520	3.60	1.06	5.60	0.040	0.676	0.041	0.128	0.830	0.128

so that (12) reduces to

$$\delta_l = -\alpha \sum_{i=1}^{3} a_i K_0(u_i). \tag{15}$$

For the same potential, (3) becomes

$$\delta_l^0 = -\alpha \sum_{i=1}^{3} a_i Q_l\left[1+\frac{1}{2}\left(\frac{b_i}{ka}\right)^2\right]. \tag{16}$$

The Q_l's were computed for $0 \leqslant l \leqslant 10$, using the polynomial expansions,[13] for $l \geqslant 10$ they were evaluated using Watson's relation[14]

$$Q_l(\cosh\xi) \sim (\exp[-(l+\tfrac{1}{2})(\xi-\tanh\xi)])(\operatorname{sech}^{\frac{1}{2}}\xi) \times (K_0[(l+\tfrac{1}{2})\tanh\xi])+O(e^{-l\xi}/l). \tag{17}$$

At $l=10$, (17) gave values in excellent agreement with the exact values and therefore its use was justified for higher l. When computing the phases for large l ($\geqslant 25$), only the term for $i=3$ is of importance in (7). Since the corresponding ξ is much less than unity, (17) reduces very nearly to

$$K_0[(l+\tfrac{1}{2})\xi] = K_0[(l+\tfrac{1}{2})(b_3/(ka))],$$

so that the δ_l's and δ_l^0's are in close agreement.

Corresponding quantities for the F potential (8) can be readily obtained: Integrals involving a term of the form $cre^{-\beta r}$ are obtained by differentiating with respect to β the integrals already obtained for terms of the form $ce^{-\beta r}$ (the U potential).

The Scattering Amplitudes

In summing (1), the convergence of the real part is improved by subtracting $f^B(\theta)$ as given by its series expansion (2) and adding it as obtained by the integration of (4). The integrated expressions are respectively, for U and F,

$$f^B(\theta) = -2k\alpha a^2 \sum_{i=1}^{3} a_i (b_i^2+a^2s^2)^{-1}, \tag{18}$$

and

$$f^B(\theta) = -2k\alpha[(\beta_1^2+s^2)^{-1}+(2c\beta_2)(\beta_2^2+s^2)^{-2}]. \tag{19}$$

By substituting the following asymptotic expressions:[15]

$$K_0(x) \sim (\tfrac{1}{2}\pi/x)^{\frac{1}{2}}e^{-x}, \tag{20}$$

and

$$P_l(\cos\theta) \sim \sqrt{2}(\pi l \sin\theta)^{-\frac{1}{2}} \sin[(l+\tfrac{1}{2})\theta+\pi/4] \leqslant \sqrt{2}(\pi l \sin\theta)^{-\frac{1}{2}}, \tag{21}$$

into the respective expressions for the real and the imaginary parts of $f(\theta)$, it was shown that negligible errors would arise from termination of the summation at $l=70$ for the real part and at $l=100$ for the imaginary part, for $\theta \gtrsim 1°$. For $\theta=0°$, $P_l(\cos\theta)=1$ and an exact termination correction can be made.

The $P_l(\cos\theta)$ were obtained from the available tables up to $l=10$ and for $10 \leqslant l \leqslant 100$, $1° \leqslant \theta \leqslant 16°$, they were computed from the relation

$$P_l(\cos\theta) \sim (\theta/\sin\theta)^{\frac{1}{2}} J_0[(l+\tfrac{1}{2})\theta] \tag{22}$$

which may be derived from the corresponding asymptotic expressions.[16] Equation (22) was satisfactory for l as low as 5 over the whole range of θ indicated in Table II.

TABLE III. Values of s where $\eta_U(\theta)-\eta_F(\theta)=\pi/2$.

Voltage, kev	s_{observed}	$s_{\text{partial waves}}$	$s_{\text{2nd Born}}$
40	10.7±0.6	10.9	7.7
11	6.6±0.6	7.1	3.8

[13] A. Cayley, Messenger Math. **17**, 21 (1887). The same polynomials with decimal coefficients are given by N. Rosen, Phys. Rev. **38**, 255 (1931).

[14] G. N. Watson, Messenger Math. **47**, 151 (1918).

[15] See, for example, E. Jahnke and F. Emde, *Funktionentafeln* (Dover Publications, New York, 1945), fourth edition, p. 138, noting that $K_0(x)=(\pi/2)iH_0^{(1)}(ix)$, and p. 117.

[16] Reference 15, pp. 117, 138; see also reference 7, p. 144.

Atomic Scattering Amplitudes for Electron Diffraction*

By James A. Ibers** and Jean A. Hoerni

Gates and Crellin Laboratories of Chemistry,
California Institute of Technology,***
Pasadena, California, U.S.A.

Scattering amplitudes for 40 kev electrons have been computed from the partial waves scattering theory for selected atoms and for scattering angles between 0° and 28°. The Thomas-Fermi potential was used in these calculations; in some instances, Hartree potentials were also used and the results from the different potentials are compared.

1. Introduction

The atomic scattering amplitudes $f(\theta)$ which are required in the electron diffraction determination of the molecular structure of gases have in the past been estimated by the first Born approximation,

$$f(\theta) \approx f^B(\theta) = \frac{2k\alpha}{Ze^2} \int_0^\infty V(r) \frac{\sin sr}{sr} r^2 dr. \qquad (1)$$

---

* This work was supported in part by the U. S. Office of Naval Research.

** General Electric Company Predoctoral Fellow, 1953-1954.

*** Contribution No. 1869. Accepted for publication in Acta Crystallographica, 1954.

Here k is $2\pi/\lambda$, α is $-Ze^2/\hbar v$, s is $2k \sin(\theta/2)$, θ is the scattering angle (twice the Bragg angle), and $V(r)$ is the potential energy of the incident electron in the atomic field. The x-ray form factor $F(\theta)$ is related to $f^B(\theta)$ by

$$f^B(\theta) = (-2k\alpha/s^2)\,(1 - F(\theta)/Z). \qquad (2)$$

Recent work (Schomaker & Glauber, 1952; Glauber & Schomaker, 1953) has shown that the first Born approximation, which is theoretically justified only for $-\alpha \to 0$, fails at the voltages used in electron diffraction studies and leads, for example, to apparent asymmetry in the structures of molecules containing both heavy and light atoms. The atomic scattering amplitude actually is complex and, on the assumption that the molecular amplitude is simply a superposition of atomic amplitudes, the intensity scattered by a molecule is proportional to

$$\sum_{i,j}{}' \left|f_i(\theta)\right| \left|f_j(\theta)\right| \cos\{\eta_i(\theta) - \eta_j(\theta)\} \frac{\sin sr_{ij}}{sr_{ij}} \qquad (3)$$

where $\eta(\theta) = \arg f(\theta)$ and r_{ij} is the distance between atoms i and j. Complex atomic scattering amplitudes have recently been computed by the partial waves scattering theory for U and F atoms at 40 and 11 kev, and the scattering of the UF_6 molecule, predicted from these results, was found to be in good agreement with experiment (Hoerni & Ibers, 1953). In this paper we extend these calculations to other atoms and to a wider range of scattering angles at 40 kev.

2. Theory

The solution to the problem of elastic scattering of a beam of particles by a central potential is given by

$$f(\theta) = (2ik)^{-1} \sum_{\ell=0}^{\infty} (2\ell+1)\,(e^{2i\delta_\ell} - 1)\, P_\ell\,(\cos\theta). \qquad (4)$$

When $\delta_\ell \ll 1$, the partial phases δ_ℓ can be computed from the formula

$$\delta_\ell^{\circ} = \frac{k\alpha\pi}{Ze^2} \int_0^{\infty} V(r)\;\; J^2_{\ell+\frac{1}{2}}\;(kr)\;\; r\,dr. \qquad (5)$$

For large values of δ_ℓ we have shown (Hoerni & Ibers, 1953) that the WKB method can be applied and that there results approximately

$$\delta_\ell = \frac{k\alpha}{Ze^2} \int_{(\ell+\frac{1}{2})/k}^{\infty} V(r) \left\{ k^2 - \left(\frac{\ell+\frac{1}{2}}{r}\right)^2 \right\}^{-\frac{1}{2}} dr. \qquad (6)$$

When the atom is very light (e.g. $Z \leq 10$) the second Born approximation can be used. This approximation, which is more convenient to apply but valid only when $|f(\theta)| \approx f^B(\theta)$ and $\eta(\theta)$ is small, gives

$$\eta(\theta) = (k/4\pi f^B(\theta)) \int f^B(\underset{\sim}{k}', \underset{\sim}{k}'')\; f^B(\underset{\sim}{k}'', \underset{\sim}{k})\; d\Omega_{\underset{\sim}{k}''} \qquad (7)$$

where $\underset{\sim}{k}$ and $\underset{\sim}{k}'$ refer to the directions of incidence and scattering, respectively, and $\underset{\sim}{k}''$ is integrated over the sphere $|\underset{\sim}{k}''| = k$ (Glauber & Schomaker, 1953).

3. Procedure and Results

The choice of V(r) is limited. It would be most desirable to use the Hartree-Fock potentials for all atoms. These calculations, however, have not been carried out for neutral atoms above calcium, and above krypton the Hartree calculations have been made only for tungsten and mercury (Hartree, 1946). We have therefore adopted the Thomas-Fermi potential in the approximate form of Rozental (1936)

$$V(r) = -\frac{Ze^2}{r} \sum_{i=1}^{3} a_i e^{-b_i\, r/a} \qquad (8)$$

where $a_1 = 0.255$, $a_2 = 0.581$, $a_3 = 0.164$, $b_1 = 0.246$, $b_2 = 0.947$, $b_3 = 4.356$, and a, the screening radius, is $0.4685/Z^{1/3}$ in Å.* Equation (8) allows analytic integration of (5) and (6).

Tables 1 and 2 give the values of $\mathcal{M}(\theta)$ and $|f(\theta)|$ computed from (8) for selected values of Z and θ at 39.47 kev. (This voltage corresponds to a wavelength of 0.06056 Å, the calibration wavelength used in the UF_6 studies.) It is interesting that even for very light atoms the $\mathcal{M}(\theta)$ differ appreciably from zero. Comparison of $|f(\theta)|$ with $f^B(\theta)$, however, indicates a maximum difference occurring at high Z

---

* This form is a better approximation to the potential than the fit of Molière (1947) which we used in our previous paper.

Table 1. Values of $\mathcal{M}(\theta)$ (radians)

θ (deg)	0	1	2	4	6	8	10	12	16	20	24	28
Z												
1	0.00_5	0.01	0.04	0.06	0.07	0.08	0.09	0.10	0.11	0.12	0.12	0.13
3	0.02	0.04	0.08	0.14	0.18	0.21	0.23	0.25	0.27	0.30	0.33	0.35
6	0.03	0.08	0.14	0.23	0.30	0.36	0.41	0.44	0.51	0.56	0.60	0.64
9	0.05	0.11	0.19	0.31	0.41	0.50	0.57	0.63	0.72	0.79	0.85	0.91
12	0.06	0.13	0.23	0.39	0.52	0.62	0.72	0.80	0.92	1.02	1.10	1.16
15	0.07	0.15	0.27	0.46	0.61	0.74	0.85	0.95	1.11	1.23	1.32	1.40
18	0.08	0.17	0.31	0.52	0.70	0.86	0.98	1.09	1.28	1.43	1.54	1.63
22	0.10	0.20	0.35	0.60	0.82	0.99	1.14	1.27	1.50	1.68	1.81	1.92
26	0.12	0.22	0.39	0.68	0.91	1.12	1.29	1.44	1.70	1.91	2.07	2.20
32	0.14	0.26	0.45	0.77	1.05	1.29	1.50	1.68	1.98	2.24	2.45	2.61
38	0.17	0.28	0.50	0.86	1.17	1.45	1.69	1.89	2.24	2.54	2.78	2.98
44	0.19	0.31	0.54	0.93	1.28	1.59	1.86	2.09	2.48	2.81	3.07	3.31
50	0.21	0.33	0.57	1.00	1.38	1.72	2.01	2.26	2.69	3.05	3.35	3.62
56	0.22	0.35	0.60	1.07	1.47	1.84	2.15	2.43	2.90	3.29	3.61	3.90
62	0.24	0.36	0.63	1.13	1.57	1.95	2.28	2.58	3.08	3.50	3.85	4.16
68	0.25	0.38	0.65	1.19	1.65	2.05	2.41	2.72	3.26	3.71	4.09	4.40
74	0.26	0.39	0.68	1.24	1.72	2.14	2.52	2.85	3.43	3.88	4.30	4.63
80	0.27	0.41	0.70	1.28	1.78	2.23	2.63	2.98	3.58	4.07	4.50	4.85
86	0.28	0.42	0.72	1.32	1.84	2.31	2.73	3.09	3.73	4.25	4.68	5.07
92	0.29	0.43	0.73	1.35	1.89	2.38	2.82	3.20	3.86	4.42	4.86	5.27
98	0.30	0.44	0.74	1.38	1.94	2.45	2.90	3.30	4.00	4.58	5.04	5.46

Table 2. Values of $|f(\theta)|$ (Å)

θ (deg)	0	1	2	4	6	8	10	12	16	20	24	28
Z												
1	4.4	0.62	0.222	0.066	0.031	0.018	0.012	0.008	0.005	0.003	0.002	0.002
3	5.5	1.45	0.570	0.186	0.088	0.054	0.034	0.024	0.014	0.009	0.006	0.005
6	7.9	2.35	0.991	0.344	0.167	0.102	0.068	0.048	0.028	0.018	0.013	0.009
9	9.1	3.12	1.36	0.500	0.243	0.150	0.100	0.070	0.041	0.027	0.019	0.014
12	9.9	3.78	1.68	0.629	0.314	0.194	0.129	0.092	0.054	0.035	0.025	0.019
15	10.6	4.36	1.97	0.750	0.382	0.236	0.157	0.113	0.067	0.044	0.031	0.023
18	11.2	4.87	2.23	0.860	0.445	0.275	0.183	0.132	0.079	0.052	0.037	0.028
22	12.0	5.50	2.55	1.00	0.521	0.323	0.218	0.157	0.094	0.062	0.044	0.034
26	12.6	6.07	2.84	1.12	0.593	0.367	0.250	0.179	0.109	0.072	0.051	0.039
32	13.3	6.81	3.22	1.29	0.688	0.425	0.292	0.211	0.128	0.085	0.060	0.046
38	13.9	7.44	3.56	1.43	0.770	0.477	0.328	0.239	0.146	0.096	0.069	0.053
44	14.5	7.98	3.87	1.55	0.842	0.524	0.361	0.264	0.163	0.107	0.077	0.059
50	14.9	8.46	4.14	1.66	0.904	0.568	0.391	0.287	0.179	0.118	0.085	0.065
56	15.4	8.89	4.36	1.76	0.956	0.607	0.418	0.308	0.192	0.128	0.092	0.071
62	15.6	9.28	4.58	1.84	1.00	0.641	0.443	0.328	0.205	0.138	0.099	0.076
68	15.9	9.63	4.78	1.91	1.04	0.671	0.466	0.347	0.217	0.147	0.106	0.081
74	16.2	9.94	4.96	1.97	1.08	0.696	0.486	0.363	0.228	0.155	0.113	0.086
80	16.4	10.22	5.13	2.04	1.12	0.718	0.503	0.378	0.238	0.164	0.120	0.091
86	16.6	10.49	5.28	2.10	1.15	0.736	0.518	0.391	0.246	0.172	0.128	0.096
92	16.8	10.73	5.44	2.15	1.18	0.751	0.532	0.403	0.253	0.179	0.135	0.101
98	16.9	10.95	5.58	2.21	1.21	0.763	0.546	0.413	0.260	0.185	0.140	0.105

of only about 30% over the range of Z and θ considered.*

Some remarks are perhaps in order regarding the actual calculation. It is convenient to improve the convergence of (4) in the following way. For the real part of $f(\theta)$ we subtract term by term from (4) the series

$$k^{-1} \sum_{l=0}^{\infty} (2l+1)\, \delta_l^{\circ}\, P_l(\cos\theta) \tag{9}$$

and add $f^B(\theta)$, since substitution of (5) into (9) yields (1). For the imaginary part of $f(\theta)$ we subtract term by term the asymptotic form of $(1 - \cos 2\delta_l)$ for large l, namely $2\delta_l^2$. Using (8) we have

$$2\delta_l^2 \sim 2\alpha^2 a_1^2 b_1^{-1} \pi k a\, (l+\tfrac{1}{2})^{-1} \exp\left\{-2(l+\tfrac{1}{2})b_1(ka)^{-1}\right\} \tag{10}$$

$$= g(l+\tfrac{1}{2})$$

and we have for the resultant sum

$$\sum_{l=0}^{\infty}(2l+1)\, g(l+\tfrac{1}{2})\, P_l(\cos\theta)$$

$$= (2\alpha^2 a_1^2 b_1^{-1}\pi k a)\, e^{-b_1/ka}\left\{1 - 2\cos\theta\, e^{-2b_1/ka} + e^{-4b_1/ka}\right\}^{-\frac{1}{2}} \tag{11}$$

---

* The maximum difference for argon is about 4%: This relative reliability of $f^B(\theta)$ accounts for the satisfactory agreement found by Bartell & Brockway (1953) between the atomic form factor for argon calculated from the Hartree-Fock potential and that obtained by use of the Born approximation from electron intensity data.

When the summations are made in this way, negligible errors arise from termination of the series for both the real and imaginary parts at $\ell = 100$, except for $\theta = 0°$, but here an exact correction can be applied.

In order to check the reliability of the Thomas-Fermi potential, we have fitted the Hartree-Fock potentials for F and A and the Hartree potentials for W and Hg in the form

$$V(r) = -\frac{Ze^2}{r} \sum_i \alpha_i r^{n_i} e^{-\beta_i r} . \qquad (12)$$

Equation (12) also allows analytic integration of (5) and (7). Values of $\eta(\theta)$ and $|f(\theta)|$ for these potentials at 39.47 kev are given in Table 3. It can be seen that $|f(\theta)|$ is relatively insensitive to the potential used, except at low angles. We find, as would be expected, that the relative differences in the values of $\eta(\theta)$ computed from the Hartree potentials and from the Thomas-Fermi potential increase with decreasing Z; yet, the absolute differences do not increase. Furthermore, our limited comparison indicates that the Hartree values differ from the Thomas-Fermi values by amounts which depend somewhat on θ but relatively little on Z. Since it is the absolute error in $\Delta\eta_{ij} = \eta_i - \eta_j$, according to equation (3), which affects the accuracy of the calculation of scattered intensities, it seems best to use the Thomas-Fermi potential for all atoms rather than to use the Hartree potentials where available in conjunction with the Thomas-Fermi

Table 3. Calculations from Hartree Potentials

Z	V(r)	
9	$V(r) = -(Ze^2/r)\{1.133\ e^{-4.248r} - 0.133\ e^{-127.5r} - r(6.173\ e^{-16.51r} + 10.50\ e^{-71.43r})\}$	a
18	$V(r) = -(Ze^2/r)\{1.315\ e^{-3.923r} - 0.315\ e^{-88.25r} - r(7.874\ e^{-9.634r} + 20.21\ e^{-44.22r})\}$	b
74	$V(r) = -(Ze^2/r)\{0.1573\ e^{-1.878r} + 0.6520\ e^{-7.451r} + 0.1804\ e^{-31.56r} + 0.0103\ e^{-233.4r}\}$	c
80	$V(r) = -(Ze^2/r)\{0.1208\ e^{-1.997r} + 0.4613\ e^{-5.405r} + 0.3644\ e^{-16.33r} + 0.0536\ e^{-78.69r}\}$	d

a Brown, 1933.
b Hartree & Hartree, 1938.
c Manning & Millman, 1936.
d Hartree & Hartree, 1935.

Table 3. Calculations from Hartree Potentials
(Continued)

$\mathcal{M}(\theta)$

θ (deg)	0	1	2	4	6	8	10	12	16	20	24	28
Z												
9	0.09	0.10	0.13	0.24	0.34	0.43	0.50	0.56	0.65	0.72	0.77	0.82
18	0.14	0.17	0.24	0.47	0.66	0.80	0.93	1.03	1.22	1.37	1.51	1.63
74	0.23	0.38	0.62	1.13	1.61	2.03	2.41	2.74	3.30	3.78	4.17	4.51
80	0.28	0.41	0.65	1.18	1.69	2.13	2.52	2.87	3.48	3.95	4.36	4.72

$|f(\theta)|$

θ (deg)	0	1	2	4	6	8	10	12	16	20	24	28
Z												
9	2.1[e]	1.8[e]	1.22	0.508	0.251	0.148	0.098	0.070	0.042	0.028	0.020	0.015
18	4.8	3.8	2.28	0.825	0.423	0.265	0.184	0.135	0.080	0.054	0.039	0.029
74	15.2	8.7	4.33	1.93	1.07	0.688	0.483	0.363	0.228	0.157	0.115	0.091
80	13.4	8.6	4.80	2.01	1.10	0.705	0.496	0.375	0.236	0.166	0.122	0.097

e For very low θ, the values of $|f(\theta)|$ are uncertain due to insufficient knowledge of the asymptotic behavior of the Hartree potentials.

potential.

It is extremely difficult to give an estimate of the accuracy of the results presented in Tables 1 and 2. The actual numerical details, i.e. function values, summation, problems of convergence, etc., have all been adequately handled. We cannot be so confident of the theoretical details. No corrections have been made for polarization, electron exchange, or electron spin. The first two effects are presumably important only at very low ℓ and the extra labor involved in the use of the Dirac equations is not justified. The WKB method is itself an approximation; however, previous investigators have found it to be reliable under comparable circumstances (Bartlett & Welton, 1941; Gunnersen, 1952). (We employ an approximate WKB equation, (6), which we have shown gives magnitudes and arguments differing by not more than about 3% from those computed from the more exact equation.*) The principal source of error in the calculation probably lies in our uncertain knowledge of the atomic potentials $V(r)$, which is in fact so uncertain as to justify all our other approximations. Altogether, we feel that Tables 1 and 2 are sufficiently reliable to allow

---

* The use of equation (6) together with the differences in the form of the approximate fit of the Thomas-Fermi potential and the use of a convergence factor for the imaginary part of $f(\theta)$ account for the differences in the values for U given here and given previously.

molecular structures, regardless of the atoms present, to be determined as accurately as is presently possible for compounds containing atoms of approximately the same atomic number. To be sure, the approximation of equation (3), i.e. the neglect of valence distortion, plural scattering, and the like, may not be adequate: Indeed it is more doubtful for the actual atomic scattering with phase shift than for that without phase shift given by the first Born approximation. In practice, however, this approximation seems to be satisfactory.

We note that complex atomic scattering amplitudes cannot generally be used to calculate the diffraction from single crystals (Hoerni, 1954). Analogous to the x-ray case (Coster, Knol, & Prins, 1930), complex f-values used in the kinematical theory may lead to different intensities for the reflections hkl and $\bar{h}\bar{k}\bar{l}$ in a crystal lacking a center of symmetry. At the same time, however, dynamical interactions arise among a number of diffracted beams in the crystal, so that even with complex f-values the range of validity of the kinematical theory is limited to extremely small crystals.

4. Extension to Other Voltages

Our results are directly applicable only for $V = V_o = 39.47$ kev. For voltages V not too different from V_o, the

following transformations might prove useful:

$$\eta(Z, \theta, V) \approx \eta(Z', \theta', V_o) \quad \text{if} \tag{13}$$

$$Z' = Z(V_o/V), \quad \sin(\theta'/2) = (Z'/Z)^{1/3} (k/k_o) \sin(\theta/2),$$

$$|f(Z, \theta, V)| \approx |f(Z'', \theta'', V_o)| \quad \text{if} \tag{14}$$

$$Z'' = Z(kv_o/k_o v)^3, \quad \sin(\theta''/2) = (Z''/Z)^{1/3} (k/k_o) \sin(\theta/2)$$

where $v_o = 1.1148\ 10^{10}$ cm/sec and $k_o = 103.75$ Å^{-1} refer to 39.47 kev. In Table 4 results computed for Z = 60 for 55 and 25 kev using (4) are compared with the values deduced from Tables 1 and 2 using (13) and (14). These transformations were suggested by the fact that they hold rigorously both for $f^B(\theta)$ and, if one assumes the simple screened-coulomb field $-Ze^2\, e^{-r/a}/r$ and the second Born approximation, for $\eta(\theta)$ (Glauber & Schomaker, 1953). The agreement exhibited in Table 4 for $\eta(\theta)$ is remarkable but we do not imply that such agreement can be obtained in all cases; the agreement for $|f(\theta)|$ is not as good but the indication is that $|f(\theta)|_{tran}$ are more reliable than $f^B(\theta)$.

We wish to thank Professor Verner Schomaker for his helpful criticism of the manuscript.

Table 4. Actual and Transformed Values for Z = 60

V	θ	$\mathcal{M}(\theta)_{act}$	$\mathcal{M}(\theta)_{tran}$	$\lvert f(\theta) \rvert_{act}$	$\lvert f(\theta) \rvert_{tran}$	$f^B(\theta)$
55	2	0.647	0.640	3.91	3.70	4.63
	8	1.91	1.92	0.506	0.470	0.644
	16	2.97	2.98	0.153	0.148	0.188
	24	3.65	3.67	0.076	0.074	0.067
25	2	0.590	0.576	5.46	5.75	6.85
	8	1.90	1.90	0.826	0.914	1.19
	16	3.08	3.09	0.274	0.294	0.373
	24	3.91	3.92	0.136	0.148	0.108

References

Bartell, L. S. & Brockway, L. O. (1953). Phys. Rev. 90, 833.

Bartlett, J. H., Jr. & Welton, J. A. (1941). Phys. Rev. 59, 281.

Brown, F. W. (1933). Phys. Rev. 44, 214.

Coster, D., Knol, K. S., & Prins, J. A. (1930). Z. Physik 63, 345.

Glauber, R. & Schomaker, V. (1953). Phys. Rev. 89, 667.

Gunnersen, E. M. (1952). Australian J. Sci. Research A5, 258.

Hartree, D. R. (1946). Rep. Progr. in Phys. 11, 113.

Hartree, D. R. & Hartree, W. (1935). Proc. Roy. Soc. (London) A149, 210.

Hartree, D. R. & Hartree, W. (1938). Proc. Roy. Soc. (London) A166, 450.

Hoerni, J. A. (1954). In preparation.

Hoerni, J. A. & Ibers, J. A. (1953). Phys. Rev. 91, 1182.

Manning, M. F. & Millman, J. (1936). Phys. Rev. 49, 848.

Molière, G. (1947). Z. Naturforsch. 2a, 133

Rozental, S. (1936). Z. Physik 98, 742.

Schomaker, V. & Glauber, R. (1952). Nature 170, 290.

Part III

Some Calculations of Atomic Form Factors

The Born amplitude $f^B(\theta)$ for electron scattering is related to the x-ray form factor $f(\theta)$ by

$$f^B(\theta) = \frac{-2k\alpha}{s^2}\left(1 - \frac{f(\theta)}{Z}\right). \qquad (1)$$

In the course of the work described in Part II, $f^B(\theta)$ was computed for argon and fluorine from Hartree-Fock potentials and for mercury and tungsten from Hartree potentials. Corresponding values of $f(\theta)$ are given in Table I.

Rather large differences between the values given in Table I and those in the literature were noted, and it was decided to compute form factors for some of the lighter atoms from the Hartree-Fock potentials. Professor Schomaker pointed out that the x-ray form factor could be obtained by direct Fourier transformation of the Hartree-Fock radial wave function, without recourse to the potential. A description of these calculations is given in the manuscript which follows.

Table I

X-ray Form Factors

s	f_{Hg}	f_W	f_A	f_F
0	80	74	18	9
1.81	71.6	65.7	14.8	7.53
3.62	59.8	55.4	10.4	5.05
7.24	42.5	39.0	6.9	2.38
10.86	32.1	28.5	5.3	1.64
14.48	25.2	22.1	3.8	1.36
18.09	20.3	17.9	2.7	1.14
21.69	16.8	15.0	2.0	0.92
28.88	12.2	11.1	1.4	0.54
36.03	9.3	8.5	1.2	
43.14	7.6	6.9	1.1	
50.20	6.2	5.8		

Some Calculations of Atomic Form Factors*

By Jean A. Hoerni and James A. Ibers**

Gates and Crellin Laboratories of Chemistry,
California Institute of Technology,***
Pasadena, California, U.S.A.

X-ray atomic form factors for carbon, nitrogen and oxygen have been computed from Hartree-Fock radial wave functions, and compared with the values previously obtained by James & Brindley, and McWeeny.

The x-ray form factor for coherent radiation is given by

$$f(\underset{\sim}{s}) = \int \rho(\underset{\sim}{r})\, e^{i\underset{\sim}{s}\cdot\underset{\sim}{r}}\, d\underset{\sim}{r} \qquad (1)$$

where $\rho(\underset{\sim}{r})$ is the electronic density of the isolated atom and $s = 4\pi\lambda^{-1} \sin\theta$ is the magnitude of the vector $\underset{\sim}{s}$ in reciprocal space. If the electronic density is spherically symmetric (1) reduces to

$$f(s) = \int_0^\infty U(r)\, \frac{\sin sr}{sr}\, dr \qquad (2)$$

---

* This work was supported in part by the U. S. Office of Naval Research.

** General Electric Company Predoctoral Fellow, 1953-1954.

*** Contribution No. 1898. This manuscript has been submitted for publication in Acta Crystallographica, 1954; the results described here were presented at the Spring Meeting of the American Crystallographic Association, Harvard University, April 5-9, 1954.

where $U(r)$ is the total radial charge density. James & Brindley (1931) (J & B) evaluated (2) for a number of atoms using the Hartree values of $U(r)$ (self-consistent field, without exchange). For other atoms, for which the Hartree field was not available, they resorted to an interpolation. These calculations have been extended to higher values of s by Viervoll & Ögrim (1949).

If the electronic density is aspherical, it is convenient to decompose (1) into the separate electronic contributions. Filled or half-filled sub-shells are spherically symmetric and can be treated as in (2), but odd p electrons, d electrons, etc. require special handling: For a p electron defined by

$$\rho_p = \left| \sqrt{\frac{3}{4\pi}} \frac{P(r)}{r} \cos\theta \right|^2 \qquad (3)$$

(where θ is the polar angle relative to the axis of the orbital and $\int_0^\infty P^2(r)\, dr = 1$), McWeeny (1951) (McW) has shown that the transform of (3) by (1) gives

$$f_p = f_p'' \cos^2\Theta + f_p^\perp \sin^2\Theta \qquad (4)$$

where Θ is the angle between $\underline{s}$ and the axis of the orbital and

$$f_p'' = (3/4\pi) \iiint P^2(r) \cos^2\theta \sin\theta\, e^{isr\cos\theta}\, dr\, d\theta\, d\phi \qquad (5)$$

$$f_p = (3/4\pi) \iiint P^2(r) \sin^3\theta\, e^{isr\cos\theta} \sin^2\phi\, dr\, d\theta\, d\phi \qquad (6)$$

McWeeny also obtains a "mean contribution" by averaging (4) over all directions:

$$\bar{f}_p = \frac{1}{3} f''_p + \frac{2}{3} f^{\perp}_p . \qquad (7)$$

Similar quantities f'', $f^{\perp}$, and $\bar{f}$ are defined for the whole atom by addition of the respective contributions of the individual electrons. McWeeny has applied these results to atoms from hydrogen to neon, using the approximate variational wave functions obtained in analytic form for the ground states by Duncanson & Coulson (1944).

Self-consistent fields, many of which even include exchange (the Hartree-Fock calculation) are now available for atoms for which there was no information when James & Brindley made their calculations. Thus it is now possible to compute f for most of the lighter atoms directly, without recourse to interpolations. It is of interest to do this for at least a few important atoms for comparison with the J & B and McW values.

We have computed $\bar{f}$ for C, N, and O from the ground-state Hartree-Fock radial wave functions $P(r)$ (Jucys, 1939; Hartree & Hartree, 1948; Hartree, Hartree, & Swirles, 1939), without recourse to f'' and $f^{\perp}$. This is possible even for aspherical atoms because $f(\underline{s})$ is a linear function of $\rho(\underline{r})$, so that averaging $f(\underline{s})$ over all orientations is equivalent to first

averaging $\rho(\underline{r})$ over all orientations and eventually applying (2)*:

$$\bar{f}(s) = \int_0^\infty \sum_{\substack{\text{all} \\ \text{electrons}}} P^2(r) \frac{\sin sr}{sr} \, dr. \qquad (8)$$

This form is convenient for numerical integration by I.B.M. methods which were available to us (Shaffer, Schomaker, & Pauling, 1946). The 1s, 2s, and 2p functions for each atom were transformed separately, and the interval of summation was in each case so small that the complete $\bar{f}$ values were unchanged (to within 0.002 electrons) when the interval was doubled in width. In Table I we give our numerical results and in Figure 1 these results are plotted up to the copper limit together with the $\bar{f}$ of McWeeny and the values of James & Brindley.

Between the copper and molybdenum limits we are in good agreement with Viervoll & Ögrim except for oxygen, where they appear to have made a slight error. In this range only the 1s electrons contribute to $\bar{f}$, so that the good agreement which we also find with the McW curves is a measure of the reliability of the Duncanson-Coulson 1s wave functions.

In the copper range it can be seen from Figure 1 that the

---

* The J & B direct values for a few aspherical atoms are presumably calculated in this way.

Table I

Values of f

s /0.5937* ($\mathring{A}^{-1}$)	$f_{C\ valence}$	$\bar{f}_C$	$\bar{f}_N$	$\bar{f}_O$
0	6.000	6.000	7.000	8.000
1	5.766	5.776	6.782	7.797
2	5.181	5.212	6.269	7.322
3	4.426	4.471	5.545	6.622
4	3.696	3.738	4.768	5.824
5	3.092	3.117	4.020	5.035
6	2.634	2.638	3.428	4.320
7	2.300	2.288	2.925	3.711
8	2.061	2.038	2.542	3.208
10	1.768	1.740	2.039	2.487
12	1.597	1.577	1.761	2.051
16	1.364	1.367	1.486	1.623
20	1.155	1.171	1.311	1.420
24	0.959	0.978	1.145	1.269
28	0.783	0.801	0.988	1.126
32	0.633	0.649	0.835	0.985

---

* $0.5937 = \frac{\pi}{10\ a_o}$, where $a_o = 0.52917$ is the ratio of the atomic unit of length to the Ångstrom.

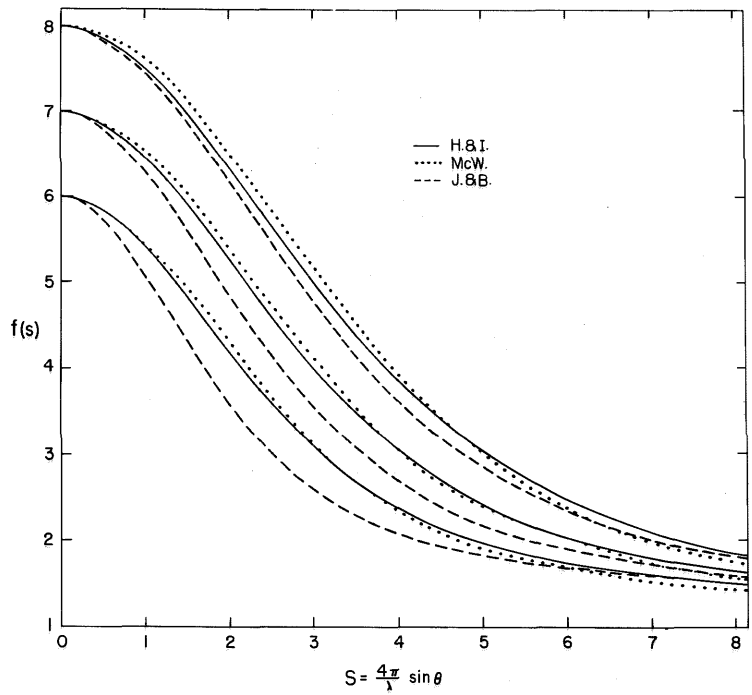

Figure 1

J & B curves are inaccurate*. Such inadequacies of the J & B curves have already been cited experimentally (Brill, 1950, Bacon, 1952). Since the J & B curve for oxygen was computed directly from the Hartree wave functions without exchange, the departure from our values is a measure of the effect of exchange.** Exchange modifies primarily the density of the outer electrons, in this case the 2s and 2p electrons. This effect is approximately the same for C, N, and C, as can be seen from comparison of exchange and non-exchange wave functions. The increasing errors in the sequence O to C are therefore due to a failure of the J & B interpolation, in which the 2s contribution was obtained for C and N by interpolation between O and Li and the 2p contribution essentially by a guess. It is therefore not surprising that the J & B curves are unreliable in the s range where the 2s and 2p contributions are appreciable.

Figure 1 also shows small differences between our curves and those of McWeeny. These differences are due to the approximate nature of the Duncanson-Coulson 2s and 2p wave functions. For C, McWeeny has shown how to calculate an approximate form factor for the valence state from ground state wave functions. We have

---

* We note that the f values given by Pauling & Sherman (1932) are in closer agreement with our values for C, N, and O within the copper range than are the J & B values.

** We have recomputed $\bar{f}$ for oxygen from the U(r) presumably used by J & B (Hartree & Black, 1933) and have found substantial agreement.

made a similar calculation with results as shown in Table I. The differences which arise between $\bar{f}$ and $f_{valence}$ are small in our work as they are in McWeeny's.*

The usual procedure in structural investigations is to employ isotropic form factors. Then any asymmetry in the electronic distribution, the anisotropy of thermal vibrations, and all other sundry effects are lumped together into asymmetric temperature factors. In this case, the use of $\bar{f}$ is a reasonable approximation and the $\bar{f}$ values deduced from the Hartree-Fock radial distributions are surely superior to McWeeny's. However, the differences do not exceed 0.2 electrons and are hardly significant in most crystal structure work. If, on the other hand, the comparatively large effects of atomic asymmetry are to be taken into account in an elaborate structure refinement, we would write:

$$f^{\parallel} = \bar{f} + \frac{2}{3}\Delta \ , \tag{9}$$

$$f^{\perp} = \bar{f} - \frac{1}{3}\Delta \ , \tag{10}$$

where $\Delta = f^{\parallel} - f^{\perp}$ can be computed from McWeeny's values. This is a sufficient approximation, since Δ is small relative to the f value for the whole atom.

---

* The McW values of $\bar{f} - f_{valence}$ are not quite smooth.

In agreement with McWeeny's work, the present work has shown that the interpolation technique of James & Brindley is unreliable. It is not unlikely that their interpolated values for other atoms as well are faulty, so that new calculations are desirable, based when possible on Hartree-Fock radial wave functions. If non-spherical effects are considered, it should be noted that, whereas (8) holds for any orbital, (4) and (7) only apply to p electrons. Corresponding expressions for d electrons, for example, can be worked out in a similar way, provided that the shape of orbital has been previously deduced from an estimate of the bonds in which the atom is engaged.

We wish to thank Professor Verner Schomaker for suggesting this problem and for his continued interest in the work.

References

Bacon, G. E. (1952). Acta Cryst. 5, 492.

Brill, R. (1950). Acta Cryst. 3, 133.

Duncanson, W. E. & Coulson, C. A. (1944). Proc. Roy. Soc. Edinb. A62, 37.

Hartree, D. R. & Black, M. M. (1933). Proc. Roy. Soc. A139, 311.

Hartree, D. R. & Hartree, W. (1948). Proc. Roy. Soc. A193, 299.

Hartree, D. R., Hartree, W., & Swirles, B. (1939). Trans. Roy. Soc. (London) A238, 229.

James, R. W. & Brindley, G. W. (1931). Phil. Mag. 12, 81.

Jucys, A. (1939). Proc. Roy. Soc. A173, 59.

McWeeny, R. (1951). Acta Cryst. 4, 513.

Pauling, L. & Sherman, J. (1932). Z. Krist. 81, 1.

Shaffer, P. A., Schomaker, V., & Pauling, L. (1946). J. Chem. Phys. 14, 659.

Viervoll, H. & Ögrim, O. (1949). Acta Cryst. 2, 277.

Part IV

Structural Studies by X-ray Diffraction

Reprinted from *Acta Crystallographica*, Vol. 6, Part 4, April 1953

PRINTED IN DENMARK

I

Acta Cryst. (1953). **6**, 367

The unit cell and space group of tetrapyridinecopper (II) fluoborate.*

By JAMES A. IBERS†, *Gates and Crellin Laboratories of Chemistry, California Institute of Technology, Pasadena, U.S.A.*

(*Received* 15 *January* 1953)

Tetrapyridinecopper (II) fluoborate, $Cu(C_5H_5N)_4(BF_4)_2$, was kindly supplied to us by Prof. James C. Warf (1952) of the University of Southern California. The deep-blue crystals exhibit primarily a columnar habit. Upon exposure to air for a few days the crystals turn light green in color, presumably owing to the loss of pyridine.

With Laue photographs prepared with a continuous spectrum of minimum wavelength 0·3 Å, and with rotation photographs prepared with copper K radiation filtered through nickel foil, we have found the crystal to be orthorhombic with

$$a = 10{\cdot}22 \pm 0{\cdot}01,\ b = 13{\cdot}87 \pm 0{\cdot}01,\ c = 16{\cdot}56 \pm 0{\cdot}01\ \text{Å}.$$

On Weissenberg photographs made with filtered copper radiation even orders from the respective pinacoids were observed up to $h = 12$, $k = 16$, and $l = 18$, but no odd orders were observed. Reflections of all other types were present. Hence the space group is probably D_2^1–$P2_12_12_1$. No piezoelectric effect, however, could be observed. The density measured pycnometrically was 1·55 g.cm.$^{-3}$, whereas a density of 1·565 g.cm.$^{-3}$ corresponds to four molecules in the unit cell. The observed density is probably low because the substance is very slightly soluble in water, the pycnometric liquid.

Because of the size and the complexity of the unit cell, no further work is contemplated on this structure.

* Contribution No. 1765 from the Gates and Crellin Laboratories.

† National Science Foundation Predoctoral Fellow, 1952–1953.

Reference

WARF, J. C. (1952). *J. Amer. Chem. Soc.* **74**, 3702.

FR. BAGGES KGL. HOFBOGTRYKKERI
COPENHAGEN, DENMARK

II

Potassium Fluotitanate

Although some contrary results are reported in the literature (1), anhydrous potassium fluotitanate K_2TiF_6 was prepared quite easily by adding potassium fluoride to a hot aqueous-hydrofluoric acid solution of titanium dioxide and allowing the solution to cool. Potassium fluotitanate crystallized as very thin hexagonal plates. These plates were found to be uniaxial under the petrographic microscope and the conclusion that the substance belonged to the trigonal system was confirmed by Laue symmetry D_{3d} normal to the face.

Layer-line measurements, uncorrected for film contraction, on rotation photographs prepared with filtered copper K and filtered molybdenum K radiation indicated a c axis of 4.66 Å and an a axis of 5.70 Å. An observed density of 3.01 g/cm^3, obtained by flotation in methylene iodide-methylene bromide mixtures, agreed well with the density of 3.05 g/cm^3 calculated for one molecule in the unit cell.

Indexed a-axis and c-axis rotation photographs required a C lattice and eliminated any screw axes or glide planes. This information together with Laue symmetry D_{3d} and the orientation of the mirror planes on the Laue photograph with respect to the a axis required that the space group be C_{3v}^1, D_3^2, or D_{3d}^3. Since no piezoelectric effect was observed and since the molecule could easily have a center, the space group was assumed to be centrosymmetric, that is $D_{3d}^3 - C\bar{3}m$.

This space group allows the titanium atom to be at 000, the potassium atoms to be at $1/3,2/3,z$; $2/3,1/3,\bar{z}$, and the fluorine atoms to be arranged octahedrally ($x,\bar{x},z$; $x,2x,z$; $2\bar{x},\bar{x},z$; $\bar{x},x,\bar{z}$; $\bar{x},2\bar{x},\bar{z}$; $2x,x,\bar{z}$) around the titanium atom. It was concluded from geometrical considerations that reasonable values of these parameters would be $x = 1/8$ to $1/5$, $z \simeq 1/4$, and $Z \simeq 3/4$.

The parameters could be determined easily by a consideration of the relative intensities of selected reflections as functions in paramter space. The intensities, obtained on rotation photographs, were estimated visually. The parameter x had been determined to be 0.155 ± 0.010 when the Program of the American Crystallographic Association Meeting (1952) announced "The Crystal Structure of K_2TiF_6" by Stanley Siegel. Correspondence with Dr. Siegel (of Argonne National Laboratory) confirmed the results to date, and so work was discontinued.

Dr. Siegel's results (2) are:

Trigonal: $a = 5.715 \pm 0.002$ Å, $c = 4.656 \pm 0.001$ Å;

$\rho = 3.07$ g/cm^3; $Z = 1$. Space group D_{3d}^3-$C\bar{3}m$:

$x = 0.156 \pm 0.003$, $z = 0.244 \pm 0.004$, $Z = 0.700 \pm 0.004$.

References

(1) H. Ginsberg and G. Holder, Z. anorg. u. allgem. Chem. 190, 407 (1930); ibid, 196, 188 (1931); ibid, 201, 193 (1931). A. King, "Inorganic Preparations," (D. Van Nostrand Co., New York, 1936), p. 127.

(2) S. Siegel, Acta Cryst. 5, 683 (1952).

III

A Preliminary Report on the Structure of Monoclinic Ceric Iodate

A. Introduction

A thorough and accurate determination of the structure of ceric iodate is of interest for several reasons: there are no accurate data available on an iodate structure; there is, in these times, a growing interest in rare-earth compounds and their structures; there is a need for the application of modern structure methods to inorganic compounds.

Only two iodate structures have been studied by single-crystal techniques. Iodic acid was studied by Rogers and Helmholz (1) in 1941. The structure was determined from Patterson and Fourier projections, based almost exclusively on equatorial data obtained with molybdenum radiation. The structure is built up of distorted IO_6 octahedra. I-O distances of 1.80, 1.81, and 1.89 Å were found. Sodium iodate was studied by MacGillavry and van Eck (2) in 1943. A previous investigation by Zachariasen (3) provided the sodium and iodine positions; Fourier projections, based on equatorial data obtained with molybdenum radiation, led to a structure which may be described as a distorted cesium chloride packing of sodium ions and iodate ions. I-O distances of 1.80, 1.80, and 1.83 Å were found. Sodium iodate was also studied by Náray-Szabó and Neugebauer (4) in 1947. Only a very limited number of intensities obtained with copper radiation were used. Systematic variation

of the parameters led to a structure in agreement with the one of MacGillavry and van Eck, except that I-O distances of 2.05, 2.05, and 2.08 Å were found. This discrepancy in the I-O distances of sodium iodate is not too surprising in view of the very limited number of data used in the determinations.

Thus, there is very little information on iodate structures and on the I-O distance. Moreover, only structures of iodates of the general formula MIO_3 have been studied. Ceric iodate, with four iodate groups per molecule, is thus of added interest.

Cerium compounds are quite frequently isomorphous with plutonium compounds. The isomorphism of rare-earth and transuranic compounds is quite common; in fact, structures of transuranic compounds are most conveniently determined by studies of the isomorphous rare-earth compounds. Naturally, the chemistry of both the rare-earth and transuranic compounds is of great interest today.

Because of the expense and the labor involved, complete three-dimensional structure determinations, which employ modern methods and techniques (the three-dimensional Patterson, Fourier, and least-squares), have been limited almost entirely to organic compounds of biological interest. It is contended that these modern methods are of general applicability and that this general applicability can be hidden by the overspecialization of the

problem. The application of these modern methods to inorganic structures is of value then, if for no other reason than to prevent stagnation of thought and technique.

A tetragonal form of ceric iodate (with $a = 9.877$ Å, $c = 5.259$ Å, $\rho = 5.4$ g/cm^3, $Z = 2$) has been reported by Staritzky and Walker (5) of Los Alamos Scientific Laboratory. Correspondence with Dr. Staritzky established that no further work was contemplated on the structure and that no sample was available. It was suggested that Professor H. H. Willard of the University of Michigan, who prepared the ceric iodate for Los Alamos, might be able to supply an additional sample. Professor Willard had no sample on hand, but he immediately prepared about twenty grams of ceric iodate. Optical goniometry and Laue photographs indicated that this sample of ceric iodate was monoclinic rather than tetragonal. A powder photograph of the monoclinic form was prepared and sent to Los Alamos. Dr. W. Burton Lewis (6) of Los Alamos examined the photograph and reported that it showed no similarity to the powder photograph which he had of the tetragonal form. Dr. Lewis also expressed an interest in ceric iodate and the isomorphous plutonium iodate and suggested that his group might look into the preparation and structure of the tetragonal form in conjunction with the study at the California Institute of the monoclinic form. Dr. Don Cromer (7) of Los Alamos reports that the tetragonal form has been prepared and that a structure determination will begin

during the summer of 1954.

Optical goniometry and Laue photographs indicated that the ceric iodate on hand was monoclinic with a β angle of $97\frac{1}{2} \pm \frac{1}{2}^{o}$. Weissenberg and rotation photographs taken with copper K radiation filtered through nickel gave for the edges of the unit cell $a = 9.56 \pm 0.05$ Å, $b = 14.90 \pm 0.07$ Å, $c = 8.05 \pm 0.04$ Å. Extinctions required the space group to be C_{2h}^{5}-$P2_1/n$. The observed density of 4.87 ± 0.04 g/cm^3 agreed well with the density of 4.91 ± 0.07 g/cm^3 calculated for four molecules in the unit cell.

B. The Collection and Estimation of Intensity Data

1. The preparation of the specimen.--- Ceric iodate has a linear absorption coefficient for copper Kα ($\lambda = 1.5418$ Å) of 1270, for molybdenum Kα ($\lambda = 0.7107$ Å) of 159 (8). One habit of monoclinic ceric iodate is equant, and a calculation of absorption for a cube 0.006 cm on an edge gives values of A, the ratio of intensity with absorption to intensity without absorption, of 0.38 for molybdenum Kα normal to a face and Bragg angle 0^{o} to 0.48 for molybdenum radiation along a face diagonal and Bragg angle 90^{o}*. Corresponding values of A for copper Kα are 0.0005 and 0.088. Reliable intensity data can thus be obtained only with

---

* These calculations were made only for a few geometrically simple cases, and there is no reason to believe that the maximum range of values of A has been found.

molybdenum radiation on a cylindrical or spherical crystal where exact absorption corrections can be made. A grinder patterned after the design of Bond (9) readily reduced crystals of ceric iodate to near-perfect spheres. A sphere with a maximum diameter of 0.0097 cm and a minimum diameter of 0.0091 cm was selected for use in the intensity work and was mounted with silicone grease on the end of a very thin glass rod. Laue photographs used for orientation purposes showed that the crystal was of excellent quality.

2. The preparation of the x-ray photographs.--- Weissenberg photographs were taken with molybdenum radiation from a North American Philips Company type 32067 (20 ma, 50 KVP) x-ray tube. A strip of zirconium metal 0.038 mm thick was placed between the layer-line screen and the film to filter the molybdenum radiation and particularly to remove the fluorescent cerium-L and iodine-L radiation. The film radius was $90/\pi$ mm. Exposures of about 2000 ma-hrs gave data out to $\sin\theta/\lambda$ of 1.0. (θ, the Bragg angle, is one half the angle between the incident and scattered beam.) The entire volume of the reciprocal lattice which lies within $\sin\theta/\lambda \leq 1.0$ contains about 9,600 points; it was covered by photographs around two axes up to an equi-inclination angle μ of 30°. Data were thus collected from the reciprocal lattice nets $0 \leq h \leq 13$, $0 \leq l \leq 11$. The multiple film technique was used: copper sheets 0.025 mm thick were placed between successive films

to increase the film factor and to reduce the total number of films necessary to five. The camera would hold conveniently only three films and two sheets of copper. Thus, for each layer, in addition to the 2000 ma-hr exposure, a short exposure of about 100 ma-hrs was necessary.

3. The preparation of the intensity strip and the estimation of intensities.---- Intensities were estimated visually with the aid of an intensity strip. Densitometer tests indicated that a change in photographic density of about 5% could be detected except at very low density. The intensity strip was therefore constructed so that successive spots were related approximately by $I_j = (I_{j+1})^{0.95}$; the intensities ranged from 1 to 100, and the weakest spot was barely visible. The 080 reflection was used in the preparation of the strip although almost any reflection of suitable intensity could have been used since the very small spherical crystal gave round reflections of uniform size. Intensities were estimated with the Weissenberg photograph on a light box, the intensity strip on top of the photograph, and a simple magnifier of power 3X mounted about 4 cm from the films. The compressed side of the Weissenberg photograph was measured. The estimated intensities from a given layer were recorded in rows and columns on a data sheet, rows corresponding to constant k, columns to constant h or ℓ. About 150 reflections per hour could be estimated. Although intensities were estimated in the range of

scale of 2 to 80, only those found to be between 7 and 60 were used in the calculation of film factors.

Table I summarizes the film factor data. In Table I f^a_{12}, for example, is the film factor between the first and second films of a particular layer (n) around the a axis. Each value of f_{12} in the table is the average of perhaps a hundred observations, f_{23} is the average of perhaps sixty observations. The quantities f_{34}, f_{45}, and f_{56} are based on a much smaller number of observations and are not given in Table I.

C. The Reduction of the Observed Intensities to $|F|^2$

1. Introduction.--- The reduction of the observed intensities to $|F|^2$ may be thought of as a three-step process. In the first step, the observed intensities are corrected for absorption and extinction and modified by Lorentz and polarization factors. In the second step, these reduced intensities are used to determine appropriate factors which bring the different reciprocal lattice nets to the same relative scale. This is usually called the correlation procedure. In the third step, the intensities, now on the same relative scale, are multiplied by a scale factor k which converts them to $|F|^2$. The scale factor is usually determined from Wilson's statistical method (10).

To make possible this reduction of the large number of intensity data for monoclinic ceric iodate, full use had to be made of punched card methods. The procedures used are described in detail below.

Table I. Film Factor Data*

n	f_{12}^{a}	f_{23}^{a}	f_{12}^{a} **	f_{23}^{a} **	f_{12}^{c}	f_{23}^{c}	f_{12}^{c} **	f_{23}^{c} **
0	3.28	3.47	3.28	3.47	3.19	3.33	3.19	3.33
1	3.19	3.43	3.19	3.43	3.25	3.29	3.25	3.29
2	3.17	3.54	3.16	3.53	3.24	3.28	3.22	3.26
3	3.28	3.84	3.26	3.81	3.25	3.44	3.22	3.41
4	3.29	3.37	3.25	3.33	3.19	3.58	3.13	3.51
5	3.31	3.30	3.24	3.23	3.12	3.52	3.03	3.41
6	3.60	3.53	3.49	3.42	3.20	3.65	3.07	3.50
7	3.49	3.52	3.35	3.37	3.23	3.58	3.04	3.37
8	3.39	3.56	3.21	3.37	3.31	3.84	3.05	3.54
9	3.38	3.51	3.14	3.27	3.38		3.04	
10	3.47	3.68	3.17	3.36	3.58		3.13	
11	3.62		3.23		3.78		3.19	
12	3.51		3.06					
13	3.69		3.12					
Avg.:			3.23	3.42			3.13	3.40

* The average deviation of film factors for $\dot{\ell}$ and $\bar{\ell}$ is about 3%. The data in the table are averages of the $\dot{\ell}$ and $\bar{\ell}$ results.

** These f's are corrected for the obliquity factor on the assumption that for $n = 0$, $f_{12} = 3.20$, $f_{23} = 3.40$.

2. The calculation of the reduced intensity.

a. The generation of h, k, and ℓ, and the calculation of $\sin^2\theta$.---

The expression

$$\sin^2\theta = (1.406\ h^2 + 0.569\ k^2 + 1.983\ \ell^2 - 0.436\ h\ell\ )10^{-3} \quad (1)$$

may be derived for monoclinic ceric iodate (molybdenum radiation). Under the direction of Professor Schomaker, a board was wired for the I.B.M. Electronic Calculating Punch (the 604) which allowed all possible values of h, k, and ℓ within the reflecting volume of the reciprocal lattice $\sin\theta/\lambda \leq 1.0$ to be generated, and the corresponding $\sin^2\theta$ (equation (1)) to be computed in a single pass through the machine. The quantities h, k, and ℓ, and $\sin^2\theta$ were punched into columns 9-10, 11-12, 13-14, 15-19, with the sign control for ℓ in column 14. In all, 9,622 reflection cards were generated.

With the same programing of the 604, a set of solid red cards were prepared for k = 0, with the punching of $\sin^2\theta$ suppressed. In this deck, the signal deck, there is a card for each possible combination of h and ℓ.

b. The calculation of M^a and M^c.---- The quantity M^a is defined by

$$I^a = I^a_{obs.} \cdot M^a \quad (2)$$

where $I^a_{obs.}$ is the observed intensity and I^a is the reduced intensity. (The superscript "a" refers to the a axis.) M^a thus

may include the absorption and extinction corrections and the Lorentz and polarization factors.

For ceric iodate no correction was made for extinction. A relative correction was made for absorption by multiplying the observed intensities by $\alpha = A_0/A_\theta$. Values of A_θ, the ratio of intensity with absorption to intensity without absorption at Bragg angle θ, are given for spherical crystals as a function of μr, where μ is the linear absorption coefficient and r is the radius of the sphere, by Evans and Ekstein (11). Values of A_θ for a μr of 0.75 (μ = 159 cm^{-1}, $\bar{r}$ = 0.0047 cm) were obtained by interpolation. For the purposes of rapid calculation the expression

$$\alpha = 1.000 - 0.134 \sin^2\theta \qquad (3)$$

was very convenient and was sufficiently accurate within the desired angle range $0^\circ \leq \theta \leq 45^\circ$. The polarization factor and the Lorentz factor for the equi-inclination Weissenberg technique (12) may be combined to give

$$\frac{1}{L\,p} = \frac{4\cos\theta}{1+\cos^2 2\theta}\left(\sin^2\theta - \sin^2\mu\right)^{\frac{1}{2}} \qquad (4)$$

where μ is the angle of inclination. M^a may therefore be

written*

$$M^a = \frac{2\alpha \cos\theta}{1+\cos^2 2\theta} (\sin^2\theta - \sin^2\mu a)^{\frac{1}{2}} \qquad (5)$$

The factor $\cos\theta / (1+\cos^2 2\theta)$ of equation (5) was available on I. B. M. cards as a function of $\sin\theta$, for $\sin\theta$ 0.000(0.001)1.000. These cards were used in the preparation of a new deck, the J deck, which for $\sin\theta$ 0.000(0.001)0.707 contained the product $(1.000 - 0.134 \sin^2\theta) \cos\theta / (1+\cos^2 2\theta)$, (equation (3)).

$\sin\theta$ was computed from $\sin^2\theta$ by use of the standard 604 square-root board, and was punched in columns 19-21 of the reflection cards. These cards were sorted on $\sin\theta$ and merged on $\sin\theta$ with the J deck. In one pass through the 604 M^a was then computed: $\sin^2\mu^a = (h\lambda/2a)^2$ was computed and subtracted from $\sin^2\theta$, the square root of this difference was taken in three iterations, and the result was multiplied by 2 and then by the combined absorption-angle factor which had been read from the appropriate J card. The quantity M^a was punched in columns 22-24. In a second pass through the 604, the quantity M^c was calculated and punched in columns 25-27.

---

* M^a is written so that its maximum value is less than unity, and therefore a column on the reflection card is saved for other information.

c. The hand-punching of the observed intensities.--- The following procedure was used to hand-punch the observed intensities onto the reflection cards. The signal deck was placed behind the reflection deck and the cards were sorted on k, ℓ, h. Because the cards were to be placed face up in the hopper of the key punch, they were removed from the sorter in reverse order after each sort; that is, the 9's were picked up before the 0's. The sorted cards were then placed in the hopper of the key punch, and $I^a_{obs.}$ was punched into columns 1-4. A signal card was in front of each new h,ℓ group of reflection cards. The observed intensities thus were read successively down a column of constant ℓ on the data sheet and punched until a red signal card appeared, and then the intensities were read from the top of the next column. The signal cards eliminated the need for close observation of the individual h, k, ℓ indices and considerably increased the speed of the punching process. The values of $I^a_{obs.}$ were listed from the cards and checked against the values on the data sheets; any errors were corrected. The cards were next resorted on k, h, ℓ, and the same procedure was then used to punch $I^c_{obs.}$ into columns 5-8. In this operation a skip bar was used which automatically reset the carriage of the key punch to column 5 after a card was ejected. Finally, the values of $I^c_{obs.}$ were listed and checked.

The following code punches were used in the hand-punching

operation: X in 1 (or 5), intensity observed to be 0; X in 3 (or 7), intensity not observed; that is, reflection was required to be absent by the space group, was hidden by the beam-stop, or was so situated in the reciprocal lattice net that it could not be obtained on a photograph around the particular axis.

d. The calculation of I^a, I^c, and R.--- The reflection cards were separated on the collator into the following groups:

Group I:	NX (no X) in 3 and 7	7,011 cards
Group II:	NX in 3, X in 7	1,141 cards
Group III:	X in 3, NX in 7	1,194 cards
Group IV:	X in 3 and 7	277 cards.

The reduced intensities I^a and I^c (equation (2)) were calculated for the Group I cards in a single pass through the 604 and were punched into columns 40-43 and 44-47. At the same time the quantity R, defined by

$$R = I^a/I^c, \tag{6}$$

was calculated and punched into columns 48-50. An X in 1 or 5 suppressed the punching of R.

3. The correlation procedure.

a. Correlation.--- The Group I cards were tabulated: h, k, ℓ, I^a, I^c, and R were listed from each card; control breaks were set on h,ℓ so that a card count and ΣR were printed for

each $h_i k \ell_j$ group. However, a card with an X in 1 or 5 did not list and did not contribute to the card count or to the sum.

The R's in each group were examined and if there were no large discrepancies ΣR was divided by the card count to give R_{ij}, the average ratio of reduced intensities for the ith a-layer to those for the jth c-layer. If there were discrepancies, these were arbitrarily removed from the calculation of R_{ij}.

The problem is to obtain values of H_i and L_j, where H_i, for example, is the factor which brings the ith a-layer to a common intensity scale. First approximations to H_i and L_j were obtained from the relations

$$\frac{H_m}{H_n} = \sum_j \frac{R_{mj}}{R_{nj}} \simeq \frac{\sum_j R_{mj}}{\sum_j R_{nj}} ; \qquad \frac{L_p}{L_q} = \sum_i \frac{R_{ip}}{R_{iq}} \simeq \frac{\sum_i R_{ip}}{\sum_i R_{iq}} \tag{7}$$

The two sets of sums $\sum_j R_{ij}$ and $\sum_i R_{ij}$ were computed and each set was reduced in scale by assigning the value 1.00 to its smallest member. The proportionality factor between $\sum_j R_{ij}$ (H_i) and $\sum_i R_{ij}$ (L_j) was determined by a limited comparison with the observed R_{ij}. The H_i and L_j were refined by a cyclic process until the changes which resulted were thought to be consistent with the accuracy of the data. (The average value of $|(R^+_{ij} - R^-_{ij})| / \bar{R}_{ij}$ was about 0.06, where the "+" refers to $\ell \geq 0$ and the "-" refers to $\ell < 0$. The average

value $\bar{R}_{ij}$ was used in the calculation of H_i and L_j.)

b. The adjustment of the intensities to the same relative scale.---

Master cards were prepared with h (or ℓ) and the corresponding H_i^{-1}(or L_j^{-1}). The signal deck was sorted on ℓ, h and then collated to select equals. (Equals arise when the sign of ℓ is disregarded.) The unselected cards were merged with the h-master cards and the values of H_i^{-1} were gang punched onto the signal cards. Similarly, values of L_j^{-1} were gang punched. The signal deck, which now consisted of one card for each possible combination of h and $|\ell|$, was merged with the Group I reflection cards. The quantities I and $\Delta I/I$, defined by

$$I = \frac{I_h + I_\ell}{2}, \quad \frac{\Delta I}{I} = \frac{|I - I_h|}{I} \tag{8}$$

where

$$I_h = I^a_{obs}.M^a H_i^{-1}, \quad I_\ell = I^c_{obs}.M^c L_j^{-1} \ * \tag{9}$$

were computed on the 604 and punched into columns 51-54, 55-57 on the reflection cards. An X in 1 or 5 suppressed the punching of $\Delta I/I$.

Similar calculations were made for Group II ($I = I_h$) and Group III ($I = I_\ell$) reflection cards, although no $\Delta I/I$ could

---

* I_h and I_ℓ were computed from equation (9) rather than from $I^a H_i^{-1}$ and $I^c L_j^{-1}$ in order to eliminate the accumulation of rounding-off errors.

be computed.

The collator was used to select those cards in Group IV which had I = 0 due to the requirements of the space group. There were 252 such cards. The 25 unselected cards represented those reflections which were hidden by the beam-stop. All but three of these reflections were observed and their intensities estimated on zero and first order Weissenberg photographs prepared with filtered copper K radiation. The intensities were then corrected for absorption, modified for Lorentz and polarization factors, and put on the scale of the molybdenum intensities by comparison with reflections of known intensity. The three unobserved reflections, $10\bar{1}$, $11\bar{2}$, and $20\bar{2}$, were arbitrarily assigned intensity 0.

Cards with $\Delta I/I$ greater than 0.50 were selected on the collator. There were 37 such cards. The indexing and the estimation of intensities were rechecked for these reflections. Usually, one estimation of the intensity had been made on a badly elongated spot which appeared on a high layer line. Such an estimation must be considered unreliable.

The number of cards in the various groups may now be broken down as follows:

Group I: 7,011 cards of which 4,255 have NX
in 1 or 5. The remaining cards are

distributed as: I = 0, 1,819; I = 1, 581;

I = 2, 275; I = 3, 68; I = 4, 10; I = 5, 3.

Group II: 1,141 cards. Group III: 1,194 cards.

1,286 cards in these groups have I = 0.

Group IV: 277 cards. 25 reflections are hidden by the beam-stop; 252 reflections are required by the space group to have I = 0.

It was quite easy to compute $\overline{\Delta I/I}$ as a function of I for the 4,255 reflections with NX in 1 and 5 of Group I. The cards were grouped on I, and tabulated to give n, ΣI, and $\Sigma \Delta I/I$ for each group. The results are presented in Table II. The trend indicated is expected: The higher relative error at low intensity results from the increased difficulty of estimating such intensities; the higher relative error at very high intensity results from the usual dependence of such intensities upon a single estimation of a spot on the last multiple film.

4. Wilson's method: the calculation of $|F|^2$.

a. Introduction.---Wilson's method (10) for the calculation of $|F|^2$ gives

$$\overline{|F|^2} = k\bar{I} = \overline{\left(\sum_{\substack{\text{unit}\\ \text{cell}}} f_i^2\right)} e^{-2B \overline{\sin^2\theta/\lambda^2}} \qquad (10)$$

where f_i is the x-ray form factor of the ith atom, and the

Table II. $\overline{\Delta I/I}$ as a Function of I

I	$\bar{I}$	n	$\overline{\Delta I/I}$
1		37	18.3%
2		164	20.4
3		268	19.3
4		305	17.1
5		287	13.5
6		303	13.3
7		251	11.4
8		237	11.0
9		175	10.4
10		195	10.1
11		148	8.7
12		131	9.2
13		134	7.7
14		104	7.1
15		95	6.8
16		89	8.7
17		66	6.8
18		64	7.9
19		53	8.0
20-29	23.85	417	7.8
30-39	34.00	241	7.3
40-49	43.61	127	7.8
50-59	53.94	89	5.9
60-69	63.95	62	7.8
70-79	74.15	40	7.4
80-89	83.95	37	9.7
90-99	94.00	26	11.2
100-199	137.53	91	7.7
200-299	243.07	14	10.9
300-399	357.00	2	12.5
400-499	452.00	3	10.3

$\overline{\Delta I/I}$ is 11.2%. This was reduced to 10.8% after the re-examination of the 37 reflections with $\Delta I/I \gg 0.50$.

quantities k and B are to be determined from the data. Thus, if the I's are grouped according to $\sin^2\theta$; $\bar{I}$, $\overline{\Sigma f_i^2}$, and $\overline{\sin^2\theta/\lambda^2}$ are computed for each group; and $\ln(\bar{I}/\overline{\Sigma f_i^2})$ is plotted against $\overline{\sin^2\theta/\lambda^2}$; a straight line of slope -2B and intercept -ln k should result. Multiplication of I by this k then gives $|F|^2$.

b. The form factors.--- The form factor for oxygen (McWeeny's $\bar{f}_O$ (13)) was already on cards as a function of $\sin\theta_{Cu}$, and a simple multiplication on the 604 converted $\sin\theta_{Cu}$ to $\sin\theta_{Mo}$. A set of blank blue cards was numbered from 000 to 707 on the 604. The form factor deck was sorted on $\sin\theta_{Mo}$, merged with these cards, and $\bar{f}_O$ was gang punched onto the blue cards.

Thomas-Fermi form factors for cerium and iodine are available in intervals of about 0.07 in $\sin\theta_{Mo}$ in International Tables (14). These form factors may be computed, however, with an accuracy of better than 2% from the following relation:

$$f = Z\left\{1 - a^2s^2\left(\frac{0.255}{0.246^2 + a^2s^2} + \frac{0.581}{0.947^2 + a^2s^2} + \frac{0.164}{4.356^2 + a^2s^2}\right)\right\} \qquad (11)$$

where

$$a = 0.4685/Z^{1/3}, \quad s = 4\pi\lambda^{-1}\sin\theta. \qquad (12)$$

(Equation (11) is based on Rozental's (15) approximate fit to the Thomas-Fermi potential.) Computation of f_{Ce} and f_I eliminates plotting, interpolation, and hand-punching.

The quantities f_{Ce}, f_I, and $\Sigma f_i^2/10$ $(4.8\ f_O^2 + 1.6\ f_I^2 + 0.4\ f_{Ce}^2)$ were calculated* and punched onto the blue cards. The reflection cards were sorted on $\sin\theta$, merged with the blue cards, and f_{Ce}, f_I, f_O, and $\Sigma f_i^2/10$ were gang punched into columns 28-30, 31-33, 34-35, and 36-39.

c. The calculation of k and B.--- The reflection cards were grouped according to $\sin^2\theta$, and for each group $\Sigma\sin^2\theta$, ΣI, $\Sigma\Sigma f_i^2/10$, ΣM^a, ΣM^c, n_t the total card count, and n_O the card count for $I = 0$ (X in 55) were obtained. To correct ΣI for the $I = 0$ reflections, it was assumed that since an observed intensity of 2 is barely perceptible, the average value of an unobserved reflection is 1. Thus

$$I_{unobs.} = (\overline{M^a} + \overline{M^c})/2 = \overline{M} \qquad (13)$$

and

$$\Sigma I' = \Sigma I + n_O\overline{M} \qquad (14)$$

where $\Sigma I'$ is the corrected sum. A straight line was drawn

---

* Professor Sturdivant pointed out that the effect of dispersion by the K electrons on the form factors for cerium and iodine has been neglected in this calculation. It is estimated (16) that the form factors for cerium and iodine should be reduced by about 1.2 electrons; the correction, therefore, amounts to at most 7% for $\sin\theta/\lambda \leq 1.0$.

through a plot of $\ln u = \ln (\overline{I'} / \overline{\Sigma f_i^2})$ vs. $\overline{\sin^2\theta/\lambda^2}$, and from the slope and intercept the values

$$k = 518, \quad B = 0.81$$

were obtained. The data used in this plot are given in Table III.

d. The calculation of $|F|^2/100$ and of G.--- $|F|^2/100$ is given by

$$|F|^2/100 = 5.18\ I. \tag{15}$$

The quantity G defined by

$$G = \left\{ |F|^2 - (\Sigma f_i^2)\ e^{-2B \sin^2\theta/\lambda^2} \right\}/1000 \tag{16}$$

is needed in the calculation of the three-dimensional Patterson function.

The quantity $B \sin^2\theta/\lambda^2$ was computed and punched onto the blue form factor cards. These cards were then merged with the exponential deck and $e^{-B \sin^2\theta/\lambda^2}$ was punched onto the blue cards. The reflection cards were then merged with the blue cards, and the calculation of $|F|^2/100$ and G was performed in one pass through the 604. The quantities $e^{-B \sin^2\theta/\lambda^2}$, $|F|^2/100$, and G were punched into columns 58-60, 61-64, and 65-67.

D. The Calculation of the Three-dimensional Patterson Function

1. Introduction.--- The Patterson function $P(x,y,z)$ with the

Table III. Data for the Determination of k and B

Grp.	n_t	n_0	$\overline{\sin^2\theta}$	$\bar{M}$	$\Sigma I'$	$10^3 u$
1	325	18	0.0296	0.144	20251	1.783
2	570	44	0.0765	0.241	20050	1.569
3	730	90	0.1261	0.321	15503	1.271
4	846	107	0.1757	0.409	12186	1,079
5	973	164	0.2253	0.500	10429	0.966
6	1064	253	0.2753	0.561	7490	0.742
7	1162	371	0.3252	0.617	6889	0.717
8	1240	522	0.3752	0.675	5276	0.580
9	1326	668	0.4253	0.706	4980	0.570
10	1386	868	0.4751	0.724	3261	0.393

peak at the origin removed may be defined as

$$P(x,y,z) = \frac{1000}{V} \sum_{h=-\infty}^{\infty} \sum_{k=-\infty}^{\infty} \sum_{l=-\infty}^{\infty} G(hk\ell) \cos 2\pi(hx + ky + \ell z) \qquad (17)$$

where V is the volume of the unit cell, x,y, and z are coordinates with respect to the axes of the lattice with magnitudes equal to fractions of the lattice dimensions, and $G(hk\ell)$ is defined by equation (16). For machine calculation, it is convenient to reduce equation (17) to a product of trigonometric functions. For the space group $P\ 2_1/n$ one obtains:

$$P(x,y,z) = \frac{4000}{V} \sum_{h=0}^{\infty} \sum_{k=0}^{\infty} \sum_{l=0}^{\infty} (A \cos 2\pi hx \cos 2\pi ky \cos 2\pi \ell z + B \sin 2\pi hx \cos 2\pi ky \sin 2\pi \ell z) \qquad (18)$$

where

$$A = G(hk\ell) + G(hk\bar{\ell}) + G(0k\ell) + G(hk0) + \tfrac{1}{2}\big(G(h0\ell) + G(h0\bar{\ell}) + G(h00) + G(0k0) + G(00\ell)\big) + \tfrac{1}{4}G(000) \qquad (19)$$

and

$$B = G(hk\bar{\ell}) - G(hk\ell) + \tfrac{1}{2}\big(G(h0\bar{\ell}) - G(h0\ell) \big). \qquad (20)$$

An estimate of the half-width in Patterson x,y,z space of an M-M peak (where M is either cerium or iodine) was made from the peak shape function $P_{ij}(r)$ defined by (17)

$$P_{ij}(r) = 4\pi \int_0^{\infty} f_i f_j \frac{\sin 2\pi Hr}{2\pi Hr} H^2 \, dH . \qquad (21)$$

In equation (21) H is $2 \sin \theta/\lambda$, and r is the radial coordinate

measured from the end of the interatomic vector between atoms i and j in Patterson space. An approximate Gaussian fit was made to the form factor for M, and the integration of equation (21) was then performed analytically. A half-width of 0.3 Å was obtained. Therefore, points will be sufficiently dense in Patterson space to enable the peak centers to be located easily if x, y, and z are varied in 1/60's (corresponding to spacings of 0.159, 0.248, and 0.134 Å).

For the monoclinic system it is only necessary to compute the Patterson function over one-fourth of Patterson space; that is, it is only necessary to extend y and either x or z to 30/60. A calculation based on this fact and on the maximum observed indices in ceric iodate ($h = 19$, $k = 29$, $\ell = 16$) indicated that the most economical order for summation was k, h, ℓ, with x and y extending to 30/60 and z to 60/60.

2. The preparation of the first-dimension cards.--- The calculation of a three-dimensional Patterson function on the M-card system devised by Professor Schomaker is described elsewhere (18). Only the procedure used in the preparation of the first-dimension cards is outlined here.

$A(hk\ell) = G(hk\bar{\ell}) + G(hk\ell)$ and $B(hk\ell) = G(hk\bar{\ell}) - G(hk\ell)$ were first computed in the following way: Two sets of blank cards

were X punched, one with the X in 2, the other with the X in 6*, and the two sets were merged. The general $hk\ell$ reflection cards ($h,k,\ell \neq 0$) were sorted on $\pm$, h, k, ℓ so that each $hk\bar{\ell}$ card was followed by the corresponding $hk\dot{\ell}$ card. (Note from equation (1) that the $hk\dot{\ell}$ card is not always present.) With the help of Dr. Louis Lavine, a collator board was wired which put an X-in-6 card and an X-in-2 card behind each $hk|\ell|$ group. A single $hk\bar{\ell}$ card was thus followed by an X-in-2 and an X-in-6 card; a single $hk\dot{\ell}$ card was an error condition which stopped the collator. Next, $B(hk\ell)$ and $A(hk\ell)$ were computed on the 604, an X in 6 caused $B(hk\ell)$ to be punched, an X in 2 caused $A(hk\ell)$ to be punched. A similar procedure was used in the calculation of $A(h0\ell)$ and $B(h0\ell)$. Each of the other groups of special reflection cards was merged with X-in-2 cards, and the calculation indicated in equation (19) was performed. However, $A(000) = G(000)/4$ was computed and punched by hand.

In the same pass through the 604 the following dummy indices h', k', ℓ' were computed and punched:

X in 2: $h' = h$, $\ell' = \ell$ X in 6: $h' = h + 20$, $\ell' = \ell + 20$

All cards: $k' = k/2$, k even
$k' = (k+81)/2$, k odd.

---

* Column 6 turned out to be a poor choice because of certain subsequent gang-punching operations in the M-card calculation.

These dummy indices are necessary for the collating operations in the M-card system and are described in detail elsewhere (18). A or B, k', h', and l' were punched into columns 2-5, 6-7, 8-9, 10-11. The cards so punched were the first-dimension cards for the calculation of the three-dimensional Patterson function.

3. The time and cards required.--- The actual calculation of the three-dimensional Patterson function required about 60 man-hours and about 75,000 I. B. M. cards.

4. The plotting of the results.--- The 54,000 calculated values of P(x,y,z) had to be plotted, of course. An x-z net was drawn on vellum backed with orange carbon paper. The x axis was drawn out to 60/60 and was divided into 1/60's. The z axis was drawn out to 30/60 and was divided also into 1/60's. The angle between and x and z axes was $\beta = 97\frac{1}{2}^{\circ}$. The scale 0.0266 $\mathring{A}$ = 1 mm was used. Copies were made from this vellum drawing by the black line process. Thirty one (y = 0/60, 1/60,...,30/60) of these copies were used in plotting the Patterson function; the plotting required about 40 man-hours.

E. The Interpretation of the Patterson Function

1. The location of the heavy atoms.--- Of the 55 heavy peaks in the Patterson, 39 were extremely well resolved. The Harker section $y = \frac{1}{2}$, the section $y = 0$, and the three single Harker peaks at 2x,2y,2z which were resolved led without difficulty to the positions of three of the heavy atoms. The positions of the two remaining

heavy atoms were then easily found. The five heavy atoms accounted for all of the observed heavy peaks. The centers of the peaks were located by interpolation, and then a cyclic procedure was used to refine the coordinates of the heavy atoms. The final coordinates are believed to be reliable to 0.001 of a cell edge; the coordinates are given in Table IV.

The next problem was to determine which of the heavy-atom positions was occupied by the cerium atom. From the coordinates and the cell dimensions, distances to nearest neighbors were computed for the five heavy atoms. These distances favor the assignment of the cerium atom indicated in Table V. (The cell dimensions are only known approximately, and therefore the distances given in Table V are probably reliable to only ± 0.05 Å.) Moreover, with the M-card system, the peak shape function (equation (21)), based on actual form factors, was evaluated for Ce-Ce, Ce-I, Ce-O, I-I, and I-O peaks. A comparison of these calculated peak shapes with those found in the Patterson function also supported the assignment of the cerium atom indicated in Table V. The peak shapes, reduced to the scale of the Patterson function, are given in Table VI.

2. The location of the oxygen atoms.--- In the Patterson function there are 50 sharp peaks of height 180-224 and 5 sharp peaks of height 90-112 which result from heavy-atom-heavy-atom interactions. There are 240 broad peaks of height 17-18 which result from

Table IV. Heavy-atom Coordinates*

Atom	x	y	z **
Ce	0.624	0.239	0.029
I_1	0.365	0.116	0.263
I_2	0.837	0.425	0.263
I_3	0.934	0.087	0.217
I_4	0.288	0.378	0.150

* The equivalent positions are x,y,z; $\bar{x},\bar{y},\bar{z}$; $\frac{1}{2}$-x,y-$\frac{1}{2}$,$\frac{1}{2}$-z; x-$\frac{1}{2}$,$\frac{1}{2}$-y,z-$\frac{1}{2}$.

** x,y,z are expressed in fractions of a cell edge.

Table V. Distances to Nearest Neighbors (Å)

Ce:			I_1:			I_2:			I_3:			I_4:		
	3.78	1		3.78	Ce		3.56	3		3.56	2		3.93	1
	3.79	2		3.93	4		3.79	Ce		3.88	Ce		3.95	3
	3.88	3		3.99	Ce		4.04	1		3.89	Ce		4.01	Ce
	3.89	3		4.04	2		4.05	1		3.95	4		4.05	Ce
	3.99	1		4.05	2		4.07	Ce		4.11	1		4.06	1
	4.01	4		4.06	4		4.12	1		4.14	1		4.14	3
	4.05	4		4.11	3									
	4.07	2		4.12	2									

Table VI. Patterson Peak Shapes*

r (Å)	Ce-Ce	Ce-I	I-I	Ce-O	I-O
0	224	201	180	18	17
0.148	181	168	149	15	13
0.296	101	92	80	9	9
0.444	34	31	29	4	4
0.592	11	11	9		
0.741	7	7	6		

*These are for doubled peaks on the scale of the Patterson. Single absolute peak shapes may be obtained by multiplying by 47.50.

heavy-atom-oxygen interactions. Therefore, the location of the oxygen atoms is a much more difficult task than the location of the heavy atoms. Knowledge of the heavy-atom positions is of considerable value, however, in the location of the oxygen atoms.

The general level of the Patterson function is perhaps 15, so that only peaks of height 30 or greater are considered to be useful. (The actual range is 30 to about 60.) All such peaks are listed, and with the help of the 604, all possible interactions of these peaks with one another are computed. If an interaction corresponds to the coordinates of a heavy-atom-heavy-atom peak, the oxygen position may be determined. That is,

$$MO = O - M, \quad NO = O - N; \therefore MO - NO = N - M = MN \qquad (22)$$

where M, N, and O symbolize the coordinates of the heavy atoms M and N and of the oxygen atom O. By this procedure, nine of the twelve oxygens in the asymmetric unit were located approximately.

Some details of the structure are now known from the heavy-atom positions and from these approximate oxygen positions. The average Ce-O distance is about 2.3 Å, the average I-O distance is about 1.9 Å. The bonding is Ce-O-I; each cerium atom is surrounded by eight nearest oxygen atoms arranged in an Archimedes antiprism. Each iodine atom is bonded to two ceriums through oxygens, but the position of the third oxygen is not known. Therefore, the coordination of oxygen atoms around an iodine atom cannot be determined.

F. Discussion

1. The work that has been done.--- The structure of monoclinic ceric iodate could not have been solved from two-dimensional projections. Two-dimensional projections together with the Harker section might have provided information sufficient for the approximate location of the heavy atoms. However, the extra week involved in the calculation of the three-dimensional Patterson function rather than just a Harker section seems insignificant in view of the five months required for the collection of the data and the estimation of intensities. Moreover, from the three-dimensional Patterson accurate heavy-atom positions and some approximate oxygen positions have been obtained.

2. The work that will be done.--- Accurate cell dimensions for monoclinic ceric iodate will be obtained.

Because the heavy-atom positions are known accurately, a three-dimensional difference Fourier, based on the inner 1,500 or 2,000 reflections where the oxygen contribution is relatively higher, should lead to the oxygen positions without difficulty. The structure can then be refined by a three-dimensional least-squares technique. It is hoped that the difference Fourier and the various refinements can be computed this summer, 1954.

References

(1) M. T. Rogers and L. Helmholz, J. Am. Chem. Soc. 63, 278 (1941).

(2) C. H. MacGillavry and C. L. P. van Eck, Rec. trav. chim. 62, 729 (1943).

(3) W. H. Zachariasen, Skrifter Norske Videnskaps-Akad i. Oslo 4, 100 (1928).

(4) I. Naráy-Szabó and J. Neugebauer, J. Am. Chem. Soc. 69, 1280 (1947).

(5) E. Staritzky and D. Walker, "Optical Properties of Some Compounds of Uranium, Plutonium, and Related Elements," LA-1439 (1952).

(6) W. B. Lewis, private communication (February, 1953).

(7) D. Cromer, private communication (April, 1954).

(8) "International Tables for the Determination of Crystal Structures," (Gebrüder Borntträger, Berlin, 1935), Vol. 2, p. 579.

(9) W. L. Bond, Rev. Sci. Instr. 22, 344 (1951).

(10) A. J. C. Wilson, Nature 150, 152 (1942).

(11) H. T. Evans, Jr. and M. G. Ekstein, Acta Cryst. 5, 540 (1952).

(12) G. Tunell, Am. Mineralogist 24, 448 (1939).

(13) R. McWeeny, Acta Cryst. 4, 513 (1951).

(14) "International Tables for the Determination of Crystal Structures," (Gebrüder Borntträger, Berlin, 1935), Vol. 2, p. 572.

(15) S. Rozental, Z. Physik 98, 742 (1936).

(16) R. W. James, "The Optical Principles of the Diffraction of X-rays," (G. Bell and Sons, London, 1950), p. 608.

(17) D. P. Shoemaker, Thesis, (California Institute of Technology, 1947), p. 82.

(18) V. Schomaker, unpublished work in this laboratory.

Part V

Propositions

1. Cox and Sharpe (1) report in addition to the trigonal form, a hexagonal and a cubic form of potassium fluotitanate, K_2TiF_6. The latter two forms were observed on an x-ray powder pattern of a sample of K_2TiF_6 which had been heated to 350°C for 24 hours and then cooled to room temperature.

It is proposed that K_2TiF_6 when heated in air to 350°C is converted, at least partially, to an oxyfluoride. Therefore, it is proposed that polymorphism in K_2TiF_6 has not been established by Cox and Sharpe.

2.(a) The Gaussian $Z(\exp(-a(Z)\ \sin^2\theta/\lambda^2))$ has been used (2,3) to represent atomic form factors. This is a very poor approximation. Furthermore, a(Z) has to be determined for each Z.

An exponential $Z(\exp(-b(Z)\ \sin\theta/\lambda))$ is proposed as an approximation to atomic form factors, with b(Z) given by a simple formula. Good agreement, in view of the simplicity of the form, is found with form factors for $\sin\theta/\lambda \geq 0.1$.

(b) In general, in order to record the values of atomic form factors on I.B.M. cards for crystal structure calculations, it is necessary to plot the available data, interpolate, and then hand-punch. It is proposed that when the Thomas-Fermi form factors are to be used, it is more convenient to calculate the values directly on I.B.M. machines from a formula based on Rozental's (4) approximation to the Thomas-Fermi potential.

3.(a) It is proposed that crystals of most substances can be ground to perfect or near-perfect spheres, and that this should be a regular procedure prior to the collection of x-ray intensity data.

(b) Two modifications of the Bond sphere-grinder (5) are proposed which make possible the grinding of very small crystals.

(c) Some suggestions are offered for the design of a goniometer head for use with spherical crystals.

4. In the course of the visual estimation of x-ray intensities on multiple films prepared with molybdenum radiation the following effects were observed: First, the film factor for the first and second films was consistently lower than the factor for the second and third films; second, the film factor was found to vary between about 3.1 and 3.4, whereas it is predicted to be around 3.8; third, the ratio of intensity on a long exposure to that on a short exposure was less than the ratio predicted from the relative times. Some partial explanations of these effects are proposed.

5. Some changes in the undergraduate chemistry curriculum at the California Institute are proposed.

6. It is proposed that the method used by Bartlett and Welton (6) and by Gunnersen (7) for summing the slowly converging partial waves series for the complex atomic scattering amplitude $f(\theta)$ is unreliable for low values of the scattering angle θ.

7.(a) A modification of the final tabulation procedure in the M-card system for the calculation of Fourier and Patterson functions is proposed. This modification would, in many cases, save considerable time in the plotting of the results.

(b) It is proposed that a great service to x-ray crystallographers everywhere would be rendered if a thorough and up-to-date description of the M-card system were published.

8.(a) The two series of compounds NO_3F, NO_2F, NOF; ClO_4F, ClO_3F, ClO_2F have not been well characterized structurally or chemically. It is proposed that these compounds be investigated (in some cases, reinvestigated) by the method of electron diffraction.

(b) Two possible methods for the preparation of ClO_2F are proposed.

9.(a) A new set of values for the atomic form factor of boron is proposed. The calculation is based on Hartree non-exchange wave functions (8) and on an extrapolation for the effect of exchange.

(b) It is proposed that an effort be made to interest someone at the California Institute in the calculation of the atomic form factors for at least the elements in the second row of the periodic table.

10. It is proposed that in the range 100 to 1,760 yards, man, the runner, decelerates at approximately 0.17 inches/seconds^2.

References

(1) B. Cox and A. G. Sharpe, J. Chem. Soc. 1953, 1783.

(2) H. L. Yakel, Jr., Acta Cryst. 7, 59 (1954).

(3) H. Lipson and W. Cochran, "The Determination of Crystal Structures," (G. Bell and Sons, London, 1953), p. 170.

(4) S. Rozental, Z. Physik 98, 742 (1936).

(5) W. L. Bond, Rev. Sci. Instr. 22, 344 (1951).

(6) J. H. Bartlett, Jr. and J. A. Welton, Phys. Rev. 59, 281 (1941).

(7) E. M. Gunnersen, Australian J. Sci. Research A5, 258 (1952).

(8) F. W. Brown, J. H. Bartlett, Jr., and C. G. Dunn, Phys. Rev. 44, 296 (1933).